

Supporting Information for

N₂O reduction at a dissymmetric {Cu₂S}-containing mixed-valent Center.

Charlène Esmieu,^{a,b,c} Maylis Orio,^d Stéphane Torelli,^{*, a,b,c} Laurent Le Pape,^{a,b,c} Jacques Pécaut,^{b,e,f} Colette Lebrun,^{b,e,f} and Stéphane Ménage^{a,b,c}

^a CNRS, UMR 5249, Laboratoire de Chimie et Biologie des Métaux, F-38054 Grenoble Cedex 9, France.
E-mail : stephane.torelli@cea.fr

^b Univ. Grenoble Alpes, F-38041 Grenoble Cedex 9, France.

^c CEA-Grenoble, DSV/iRTSV, Laboratoire de Chimie et Biologie des Métaux, F-38054 Grenoble Cedex 9, France.

^d Laboratoire de Spectrochimie Infrarouge et Raman, Bâtiment C5 - UMR CNRS 8516, Université des Sciences et Technologies de Lille, F-59655 Villeneuve d'Ascq Cedex, France.

^e CNRS, UMR_E 3, F-38054 Grenoble Cedex 9, France.

^f CEA-Grenoble, INAC, Service de Chimie Inorganique et Biologique, F-38054 Grenoble Cedex 9, France.

Table of contents

Experimental section

Figure S1. ESI spectrum of $\mathbf{L}^{\text{Me(MAM)SS}}$.

Figure S2. ESI MS-MS spectrum of $\mathbf{L}^{\text{Me(MAM)SS}}$.

Figure S3. Structures of (**C**) and (**D**) represented by thermal ellipsoids at 30 % probability.

Figure S4. DFT optimized structure of $[\mathbf{2}.(\text{H}_2\text{O})(\text{OTf})]^+$ and selected bond distances.

Figure S5. Spin-density plot (**a**) and localized SOMO (**b**) of $[\mathbf{2}.(\text{H}_2\text{O})(\text{OTf})]^+$.

Figure S6. ESI Spectrum of $[\mathbf{2}.(\text{H}_2\text{O})(\text{OTf})]^+$.

Figure S7. ESI mass spectrum of the species resulting from the addition of 1.1 molar equiv. of DABCO to a solution of $[\mathbf{2}.(\text{H}_2\text{O})(\text{OTf})]^+$ in acetone.

Figure S8. UV-Vis spectra of $[\mathbf{2}.(\text{H}_2\text{O})(\text{OTf})]^+$, $[\mathbf{2}.(\text{H}_2\text{O})(\text{OTf})]^+ + 1.1$ molar equiv. of DABCO and $[\mathbf{2}.(\text{H}_2\text{O})(\text{OTf})]^+ + 1.1$ molar equiv. of DABCO + O₂.

Figure S9. UV-Vis Spectra for crystalline $[\mathbf{2}.(\text{H}_2\text{O})(\text{OTf})]^+$ in acetone before and after add of 200 molar equiv. of NaOTf.

Figure S10. TD-DFT assignment of the calculated transitions for $[\mathbf{2}.(\text{H}_2\text{O})(\text{OTf})]^+$.

Figure S11. ¹⁹F NMR spectra for triflates-containing standards used for our study.

Figure S12. Variation of the ¹⁹F NMR shift of **[1]** and $[\mathbf{2}.(\text{H}_2\text{O})(\text{OTf})]^+$ as a function of the temperature in deuterated acetone.

Figure S13. Cyclic voltammogram for a 3.20 mM solution of $[\mathbf{2}.(\text{H}_2\text{O})(\text{OTf})]^+ + 1.1$ molar equiv. of DABCO in acetone.

Figure S14. Cyclic voltammograms for a 1.54 mM solution of $[2.\text{(H}_2\text{O)(OTf)}]^+$ in acetone without (A) and with (B) addition of excess NaOTf (200 molar equiv.).

Figure S15. X-band EPR spectra of $[2.\text{(H}_2\text{O)(OTf)}]^+$ (0.68 mM) and $[2.\text{(H}_2\text{O)(OTf)}]^+$ (0.68 mM) + 200 molar equiv. of NaOTf in acetone at 10 K.

Figure S16. X-band EPR spectra of $[2.\text{(H}_2\text{O)(OTf)}]^+ + 1.1$ molar equiv. of DABCO.

Figure S17. X-Band EPR evolution of $[2.\text{(H}_2\text{O)(OTf)}]^+$ upon progressive N_2O -bubbling in acetone at 10K.

Figure S18. (A) Composition of the headspaces gas 50 s after the start of the GC run; (B) GC profile for the reaction of $[2.\text{(H}_2\text{O)(OTf)}]^+$ (solid line) and [1] (dotted line) with N_2O showing the detection of N_2 .

Figure S19. ESI mass spectrum of the bulk solution resulting from the reaction with N_2O in acetone; (A) Experimental, (B) Calculated for the corresponding hydroxo-containing product ($[\text{LMMeMAMS}^-(\text{OH})(\text{OTf})]^+ \text{ i.e } [3.\text{(\mu OH)(OTf)}_2]$).

Figure S20. Determination of k' values according to various complex concentrations.

Figure S21. Plot of $\ln k'$ as a function of $[2.\text{(H}_2\text{O)(OTf)}]^+$ concentration to determine the reaction *pseudo*-rate order.

Figure S22. Reactivity toward N_2O of the species resulting from the deprotonation of $[2.\text{(H}_2\text{O)(OTf)}]^+$ with 1.1 molar equiv. of DABCO.

Figure S23. Calculated UV-Vis spectra for the postulated N_2O -adducts and comparison with the spectrum of $[2.\text{(H}_2\text{O)(OTf)}]^+$.

Figure S24. Spin-density plot (a) and localized SOMO (b) of (1).

Table S1. Summary of X-Ray Crystallographic Data for (**C**), (**D**), $[2.\text{(H}_2\text{O)}(\text{OTf})]^+$ and $[3.\text{(\mu OH)(OTf)}_2]$.

Table S2. Bond lengths [\AA] and angles [deg] for (**C**).

Table S3. Bond lengths [\AA] and angles [deg] for (**D**).

Table S4. Bond lengths [\AA] and angles [deg] for $[2.\text{(H}_2\text{O)}(\text{OTf})]^+$.

Table S5. Computed Metrical Parameters for $[2.\text{(H}_2\text{O)}(\text{OTf})]^+$.

Table S6. NBO analysis of the Cu-Cu bond in $[2.\text{(H}_2\text{O)}(\text{OTf})]^+$ and comparison with **[1]**.

Table S7. Optical properties of pertinent mixed-valent dinuclear copper systems.

Table S8. Predicted TD-DFT transitions (energies and intensities) and assignments for the calculated doublet state of $[2.\text{(H}_2\text{O)}(\text{OTf})]^+$.

Table S9. Bond lengths [\AA] and angles [deg] for $[3.\text{(\mu OH)(OTf)}_2]$

Experimental Section

Materials and chemicals. N_2O (purity $\geq 99.998 \%$) was purchased from Sigma-Aldrich and used without further purification. No oxygen has been detected by GC-MS. Other organic chemicals were purchased from Acros Organics, Sigma-Aldrich, or Lancaster. $[\text{Cu}(\text{OTf})(\text{CH}_3\text{CN})_4]$ is from Sigma-Aldrich. For air and moisture sensitive experiments, solvents were freshly distilled from sodium/benzophenone (THF) or calcium hydride (dichloromethane). Acroseal® purity solvents were purchased for air-sensitive experiments.

S-(2,6-bis[(bis(pyridylmethyl)amino)methyl]-4-methylphenyl)dimethylthiocarbamate (**A**) was prepared according to the published procedure.¹

Air-sensitive materials were manipulated in an Argon flushed glove box.

Instrumentation: NMR (¹H , ¹³C and ¹⁹F) spectra were acquired using a Bruker Avance 300 MHz spectrometer equipped with a QNP probehead by using deuterated solvents as reference. α - α - α trifluorotoluene served as reference for ¹⁹F chemical shifts (δ = -63.73 ppm) and for integral quantification. UV-Visible NIR spectra were recorded on a Perkin Elmer Lambda 1050 spectrophotometer operating at room temperature. For powder spectra, a Perkin Elmer Lambda 950 equipped with a 150 nm integration sphere was used. Regular UV-Visible spectra were acquired with a Shimadzu 1800 device. Mass spectrometry spectra were recorded with a Bruker Daltonics Esquire 3000 Plus (ESI-MS) device. X-band EPR spectra were obtained on a Bruker EMX spectrometer equipped with an Oxford ESR 910 cryostat for low temperature studies. The microwave frequency was calibrated with a frequency counter and the magnetic field with an NMR gaussmeter. Simulations were obtained using the EasySpin program² (4.0.0 currently developed by Stefan Stoll, California, U.S.A). For electrochemical experiments, a three-electrode setup was used. It consists in a glassy carbon (1.6 mm in diameter) disk as a working electrode, a platinum wire (auxiliary electrode) and a Ag/Ag⁺ (silver wire in 0.01 M AgNO₃ + 0.1 M tetra-N-butylammonium perchlorate in CH₃CN) reference electrode directly dipped into the solution, but isolated by a Vycor frit. Cyclic voltammograms were recorded with a EG&G PAR 273 A instrument. X-ray crystallography data were acquired at 150 K using an Oxford-diffraction XCalibur S diffractometer with graphite monochromated MoK α radiation (λ = 0.71073 Å). Molecular structure was solved by direct methods and refined on F² by full matrix least squares techniques using SHELX TL package. All non-hydrogen atoms were refined anisotropically, and hydrogen atoms were placed in ideal positions and refined as riding atoms with individual isotropic displacement parameters. The CCDC depositions numbers for (C), (D), [2.(H₂O)(OTf)]⁺ and [3.(μ -OH)(OTf)₂] are 948576, 948575, 948574 and 948577, respectively.

N₂O reduction experiments: Under an inert atmosphere, crystalline [2.(H₂O)(OTf)]⁺ in acetone (2 mL solution at 0,5 mM) was placed in a 20 mL Schlenk tube. N₂O was bubbled directly into the solution and the stirring maintained throughout the experiment. After a given time, N₂ accumulation was monitored by GC-MS (25 μ L headspace gas injection). The amount of N₂ was calculated from the GC peak area and from calibration curves. In control experiments, an identical procedure was followed in the absence of N₂O, with and without the complex, with no N₂ production observed. The yield of N₂ produced was determined based on the known amount of the starting copper complex involved in the reaction. GC/MS headspaces gas analyses were

performed using a Hewlett-Packard 6890 gas chromatograph coupled to a Hewlett-Packard 5973 mass spectrometer (Agilent Technologies). Good separation of the gaseous analytes (N_2 , O_2 , N_2O , and CO_2) was obtained using a Restek Rt®-Q-BOND column (15m x 0.53 mm x 20.0 μm) with helium as carrier gas maintained at a flow rate of 36 $\text{ml}\cdot\text{min}^{-1}$. The GC was run in the isothermal mode at 40 °C. EI mass spectra were obtained at ionization energy of 70 eV at a source temperature of 200 °C. Calibration experiments with known volumes of N_2 showed linear responses for varied molar amounts of each gas. The calibration curves used for determining the amount of N_2 evolved in the reactivity experiments were determined using injections of headspace gas samples from flasks with identical overall volumes, solvents volumes, and temperatures as those used in the N_2O reactivity experiments.

Kinetic measurements: To a 2 mL N_2O -saturated acetone solution, the appropriate volume of a stock solution of the complex was added. The reaction was followed by UV-Visible spectrophotometry. A plot of the variation of absorbance as a function of time gave the initial rate. The reaction order was obtained by plotting different reaction rates in function of complex concentrations.

Computational Details. Theoretical calculations were based on Density Functional Theory (DFT) and have been performed by the Gaussian09 package.³ To facilitate comparison between theory and experiment, full geometry optimizations were carried out using the hybrid functional B3LYP⁴⁻⁵ and the 6-31g* basis set on all atoms.⁶⁻⁷ Vibrational frequency calculations were performed to ensure that each geometry optimization converged to a real minimum. Natural Bond Order (NBO) analyses⁸⁻⁹ were performed with inclusion of the 3-center bond option in the search algorithm using the hybrid functional B3LYP in combination with the TZV/P basis set for all atoms.¹⁰ The relative energies were obtained from single-point calculations using the same functional/basis set as employed before. They were computed from the gas-phase optimized structures as a sum of electronic energy, thermal corrections to free energy, and free energy of solvation. Zero point vibrational energy (ZPVE) corrections¹¹ were evaluated from the calculated harmonic frequencies and are included in the total energies. The counterpoise (CP) procedure was used to correct the total energy for the basis set superposition error (BSSE).¹²⁻¹³ Optical properties were investigated employing TD-DFT calculations¹⁴⁻¹⁵ using the B3LYP functional together with the TZV/P basis set. Solvent effects were also included using the Polarized Continuum Model (PCM) for the case of acetone.¹⁶⁻¹⁹ EPR parameters were obtained from

relativistic single-point calculations using the ORCA program package²⁰ at the B3LYP level. Scalar relativistic effects were included with ZORA paired with the SARC def2-TZVP(-f) basis sets²¹⁻²² and the decontracted def2-TZVP/J Coulomb fitting basis sets for all atoms. Increased integration grids (Grid4 and GridX4 in ORCA convention) and tight SCF convergence criteria were used in the calculation. Visualization of the geometries, molecular orbitals and electronic densities was done with the ChemCraft program.²³ *Natural Population Analysis:* the NPA algorithm involves partitioning the charge into atomic orbitals on each centre, constructed by dividing the electron density matrix into sub-blocks with the appropriate symmetry. The NPA analysis shows two identically positive copper centers (0.97 and 1.00, respectively) and a partially negative sulfur (-0.25) matching the expectations for a fully delocalized Cu^{+1.5}Cu^{+1.5} state in [2.(H₂O)(OTf)]⁺. *Natural Bond Order Analysis:* NBO is based on a technique for optimally transforming a given wave function into localized form, corresponding to the one-center (“lone pairs”) and two centers (“bonds”) elements of the chemist’s Lewis structure picture.

[4-methyl-2,6-bis(hydroxymethyl)]-thiophenol (B) Under an inert atmosphere, solid LiAlH₄ (1.47 g, 38.6 mmol, 5 eq) was added to a stirred solution of S-(2,6-diformyl-4-methylphenyl)dimethylthiocarbamate ((A), 1.94 g, 7.72 mmol) in anhydrous THF (150 mL). The reaction mixture was refluxed for 12 h. The solution was then cooled to room temperature and 10 mL of 4 N HCl was added. The resulting biphasic mixture was stirred for 2 h, and the THF removed under reduced pressure. The aqueous phase was then extracted with AcOEt (3 x 20 mL), and the combined organic layers dried over Na₂SO₄. After evaporation of the solvent under vacuum, a beige powder was obtained (1.2 g) that was immediately engaged in the next step without purification.

[4-methyl-2,6-bis(hydroxymethyl)]-thiophenyldisulfide (C). Et₃N (1.10 mL, 7.81 mmol, 1.2 eq) was added to a solution of (B) (1.2 g, 6.51 mmol) in THF (20 mL). O₂ gas was then bubbled through the reaction mixture for 5 min and the inlet needle was removed. The resulting solution was stirred for 10 h and the solvents removed under vacuum. The crude product was washed with Et₂O (3 x 5 mL) and dried under vacuum to give a yellow solid (1.2 g, 100 %). ¹H NMR (300 MHz, MeOD): δ(ppm) 7.29 (s, 2H); 4.48 (s,broad, 4H); 2.39 (s,br, 3H). ¹³C NMR (75 MHz,

MeOD): δ (ppm) 146.9; 142.0; 128.7; 128.3; 63.0; 21.7. ESI –MS: m/z = 389.2 [$M + \text{Na}^+$]⁺. Anal.Calcd. for C₁₈H₂₄O₄S₂: C, 58.99; H, 6.05. Found: C, 59.1; H, 6.15.

[4-methyl-2,6-bis(chloro)]-thiophenyldisulfide (D). Under an inert atmosphere, a solution of SOCl₂ (2.96 mL, 41.0 mmol, 20 eq) in dry CH₂Cl₂ (20 mL) was added dropwise over a 1 h period to a stirred suspension of (C) (750 mg, 2.05 mmol) in distilled CH₂Cl₂ (20 mL) and DMF (100 μ L). After 12 h, the resulting clear solution was evaporated to dryness. The crude product was washed with Et₂O (3 x 5 mL) and dried under vacuum to give a yellow solid (850 mg, 94 %) stable only when stored at -20°C. ¹H NMR (300 MHz, CDCl₃): δ (ppm) 7.31 (s, 2H); 4.48 (s, 4H); 2.39 (s, 3H). ¹³C NMR (75 MHz, CDCl₃): δ (ppm) 142.5; 141.9; 131.7; 130.6; 44.4; 21.4. Note that the chemical shifts for both CH₂ and CH₃ @ 4.48 and 2.39 are the same as for (C). This coincidence is due to the solvents used, that are different/ The NMR spectra were recorded on single crystals for both molecules.

4-methyl-2,6-bis(N,N'-methylaminomethylpyridine)-thiophenyldisulfide L^{Me(MAM)S-S}. To a stirred solution of N,N-diisopropylethylamine (4.04 mL, 23.2 mmol, 12 eq), and [(methylamino)methyl]pyridine (1.19 mL, 9.65 mmol, 5 eq) in distilled CH₂Cl₂ (20 mL) under inert atmosphere was added a solution of (D) (850 mg, 1.93 mmol) in distilled CH₂Cl₂ (20 mL) dropwise over 1 h, at 0°C. The solution was stirred for 24 h at room temperature, after which the solvents were removed under reduced pressure. The crude oil was washed with pentane (3 x 5 mL) and dried under vacuum to give yellow oil (1.23 g, 81 %).

¹H NMR (300 MHz, CDCl₃): δ (ppm) 8.51 (d, 4H, ³J = 4.6 Hz), 7.62 (dt, 4H, ⁴J = 1.7 Hz, ³J = 7.6 Hz); 7.42 (d, 4H, ³J = 7.7 Hz); 7.27 (s, 4H); 7.12 (t, 4H, ³J = 6.2 Hz); 3.57 (s, 8H); 3.52 (broad, 8H); 2.34 (s, 6H); 2.10 (s, 12H). ¹³C NMR (75 MHz, CDCl₃): δ (ppm) 159.6; 148.7; 143.3; 139.3; 136.2; 132.3; 129.9; 122.7; 121.7; 63.5; 59.9; 42.3; 21.4. ESI –MS: m/z = 783 [$M + \text{H}^+$]⁺, Figures S1 and S2.

Anal.Calcd. for C₄₆H₅₄N₈S₂: C, 70.55; H, 6.95; N, 14.31. Found: C, 70.69; H, 7.06, N, 14.17.

[2.(H₂O)(OTf)]⁺. In a glove box, to a stirred solution of L^{Me(MAM)S-S} (121.48 mg, 0.16 mmol) in distilled acetone (2 mL) was added dropwise a solution of [Cu^I(OTf)](CH₃CN)₄ (247.19 mg, 0.66 mmol, 4.1 eq) in acetone (1.5 mL). The solution immediately turned dark violet. After stirring for 30 min, the volume was reduced to 1 mL under vacuum and diethyl ether added to precipitate a

dark solid, which was filtered to give a dark violet powder (179 mg, 67%). X-ray quality crystals were grown from layering pentane above an acetone solution of the complex. A polycrystalline powder for elemental analysis was obtained from slow evaporation of a dichloromethane solution of the complex.

UV-Vis-NIR in acetone (λ , nm; ϵ , M⁻¹.cm⁻¹): 1254 (690), 787 (735), 479 (sh, 525), 425 (sh, 670).

Anal.Calcd. for [2·(H₂O)(OTf)](OTf): C,33.93; H, 3.29; N, 6.29; Cu, 15.81. Found: C, 33.85; H, 3.24; N, 6.51; Cu, 16.11.

ESI-MS : m/z = 258.5 {[Cu₂^{L(MAM)S}]}²⁺ , m/z = 517.2 {[Cu₂^{L(MAM)S}]}⁺; 666.0 {[Cu₂^{L(MAM)S}](OTf)}⁺; 683.2 {[Cu₂^{L(MAM)S}]^{(μ-OH)(OTf)}}⁺.

[3.(μ-OH)(OTf)₂]. N₂O was bubbled in a solution of the MV mixture in acetone (20 mg, 0.024 mmol in 30 mL). The reaction was monitored by UV until no changes in the spectrum was observed. The solution was then evaporated to give a green powder (18 mg, 90 %). Single crystals suitable for X-ray diffraction analysis were obtained upon layering diisopropyl ether onto an acetone solution of the complex.

UV-Vis in acetone (λ , nm; ϵ , M⁻¹.cm⁻¹): 785 (180); 572 (390); 422 (1180).

Anal.Calcd. for [3.(μ-OH)(OTf)₂]: C,36.01; H,3.38; N,6.72. Found: C,36.27; H,3.51; N,6.85.

ESI-MS: m/z = 683.2 [Cu₂L^{Me(MAM)S}(μ-OH)(OTf)]⁺

EPR (acetone 10K, 50K or 100K): silent.

Figure S1: ESI Spectrum for $\text{L}^{\text{Me(MAM)S-S}}$

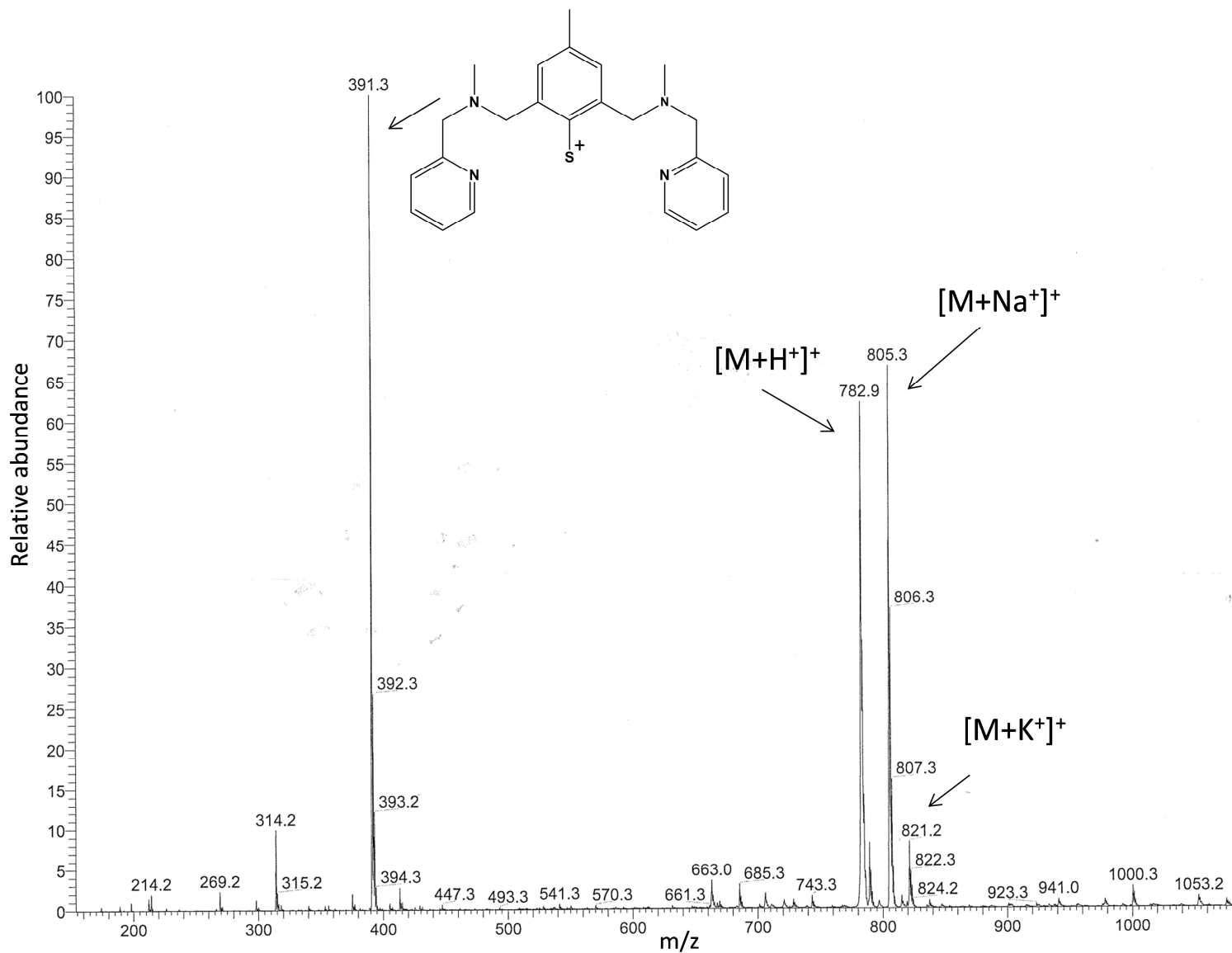


Figure S2: ESI MS-MS Spectrum for $\text{L}^{\text{Me(MAM)S-S}}$

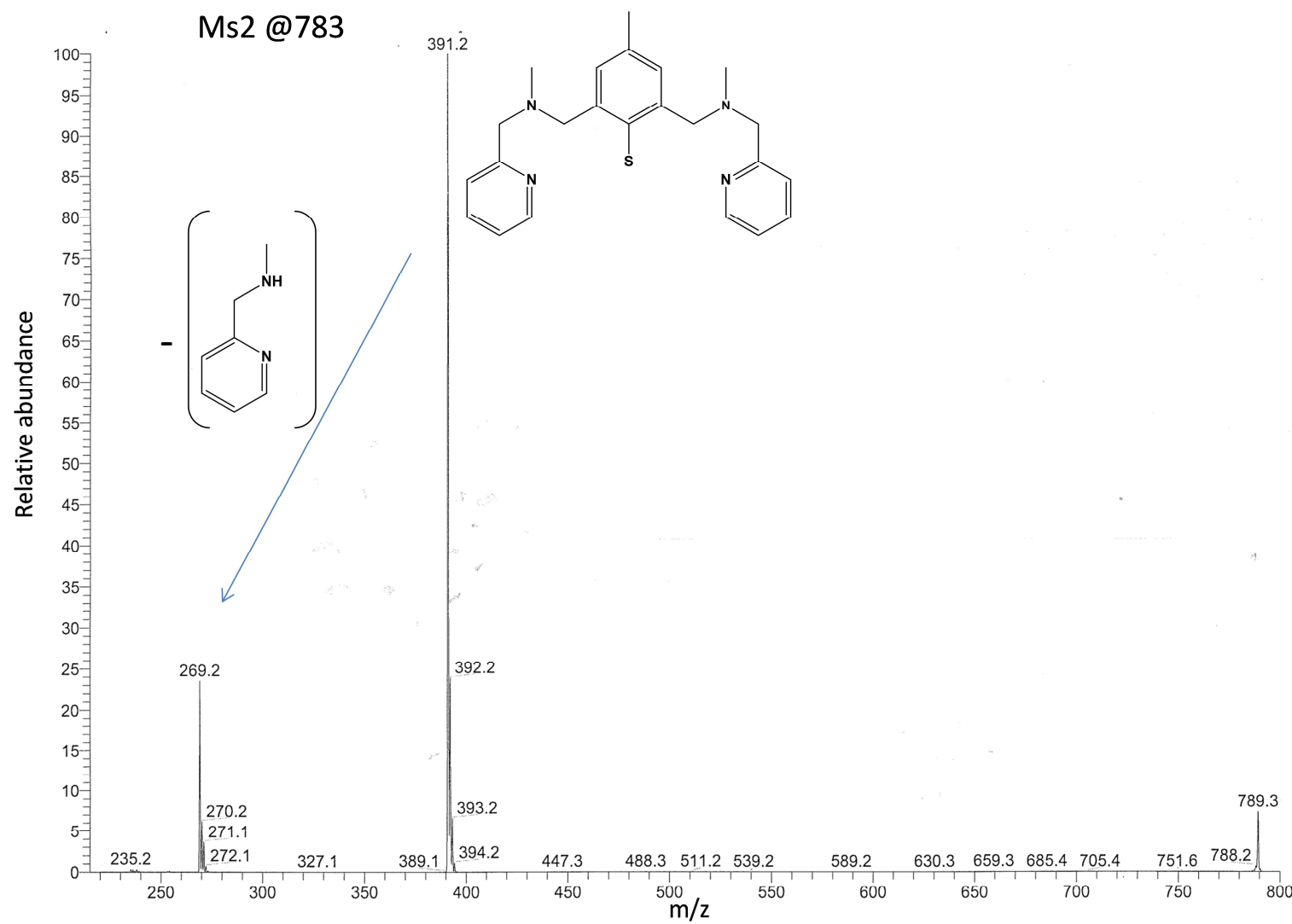


Figure S3: Structures of **(C)** and **(D)** represented by thermal ellipsoids at 30 % probability. Hydrogen atoms have been omitted for clarity. See table S3 for bond distances and angles.

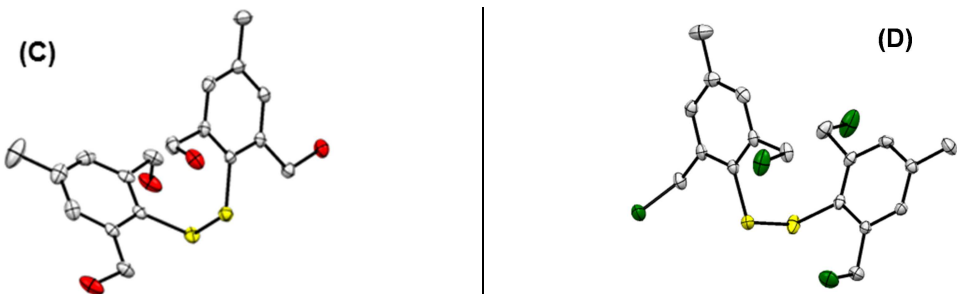


Figure S4. DFT optimized structure of $[2.\text{(H}_2\text{O)}(\text{OTf})]^+$ and selected bond distances.

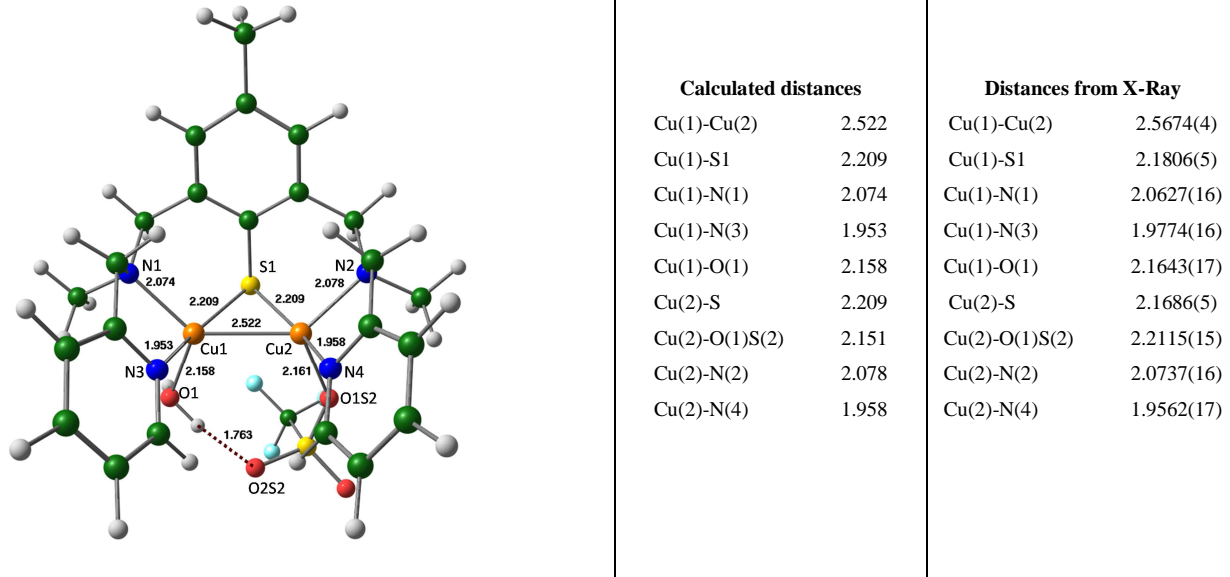


Figure S5. Spin-density plot **(a)** and localized SOMO **(b)** of $[2.\text{(H}_2\text{O)}(\text{OTf})]^+$.

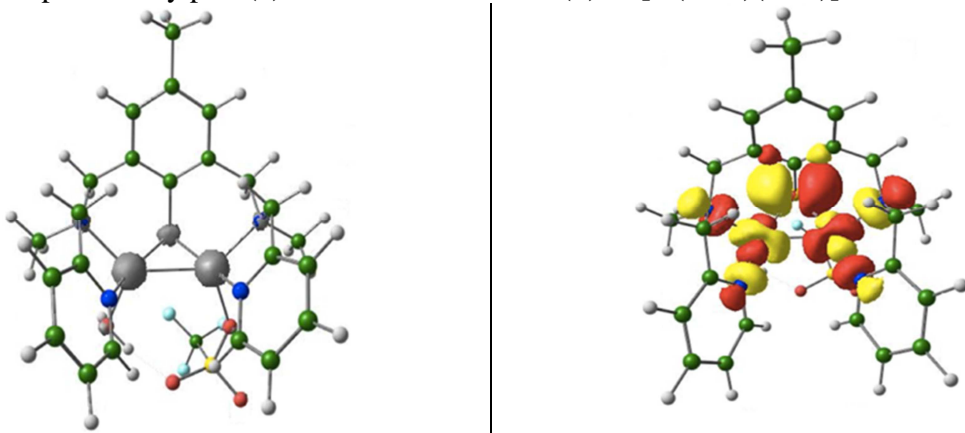
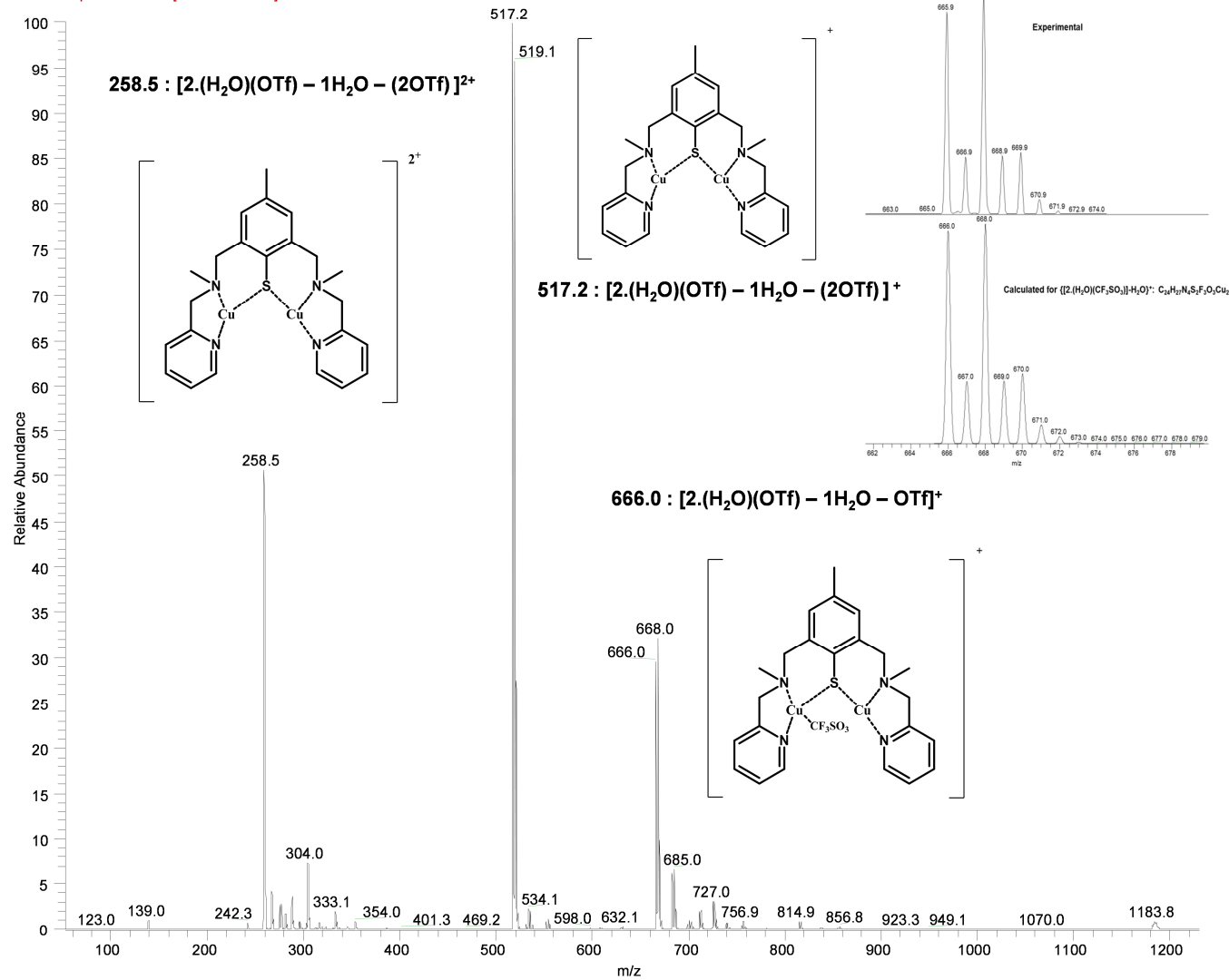


Figure S6: ESI Spectrum for $[2.\text{(H}_2\text{O)}(\text{OTf})]^+$.

LCBM 1026 #1168-1520 RT: 4.92-5.90 AV:60 NL: 1.43E5
 F: ITMS + p ESI Full ms [50.00-2000.00]



A degradation product from oxidation in air at m/z = 683.2 that was identified as $[3.\text{(}\mu\text{-OH})(\text{OTf})]^+$ was detected, together with a reduced dicuprous species at 517.2 and a dicationic MV $[2]^{2+}$ fragment at m/z = 258.5. The most significant observation is that a triflate anion can remain coordinated at a copper center.

Figure S7. ESI mass spectrum of the species resulting from the addition of 1.1 molar equiv. of DABCO to a solution of $[2.\text{(H}_2\text{O)}\text{(OTf)}]^+$ in acetone.

At first glance, the MS spectrum of $[2.\text{(OH)}\text{(OTf)}]$ is quasi-superimposable to the one $[2.\text{(H}_2\text{O)}\text{(OTf)}]^+$ but differs by one di-charged fragment @ m/z 279 (vs 258.5). Nevertheless, the full conversion of $[2.\text{(H}_2\text{O)}\text{(OTf)}]^+$ to $[2.\text{(OH)}\text{(OTf)}]$ prior to record the MS spectrum was confirmed by EPR and UV-Vis titration. Consequently, the m/z peak @ 668 is attributed to a fragmentation of $[2.\text{(OH)}\text{(OTf)}]$, resulting from the loss of an hydroxo ion and consistent with the formation of mono-charged fragment $\{\text{[2.(OH)(OTf)]-OH}\}^+$. Moreover, the di-charged peak @ 279 is tentatively assigned to a $\{\text{[2.(OH)(OTf)]-OTf-OH}^+ + \text{K}^+\}^{2+}$ ion, whereas $[2.\text{(H}_2\text{O)}\text{(OTf)}]^+$ and $[3.\mu\text{-OH}]\text{(OTf)}_2$ gave a peak at 258.5 and 267.1 respectively(Figures S19 and S6).

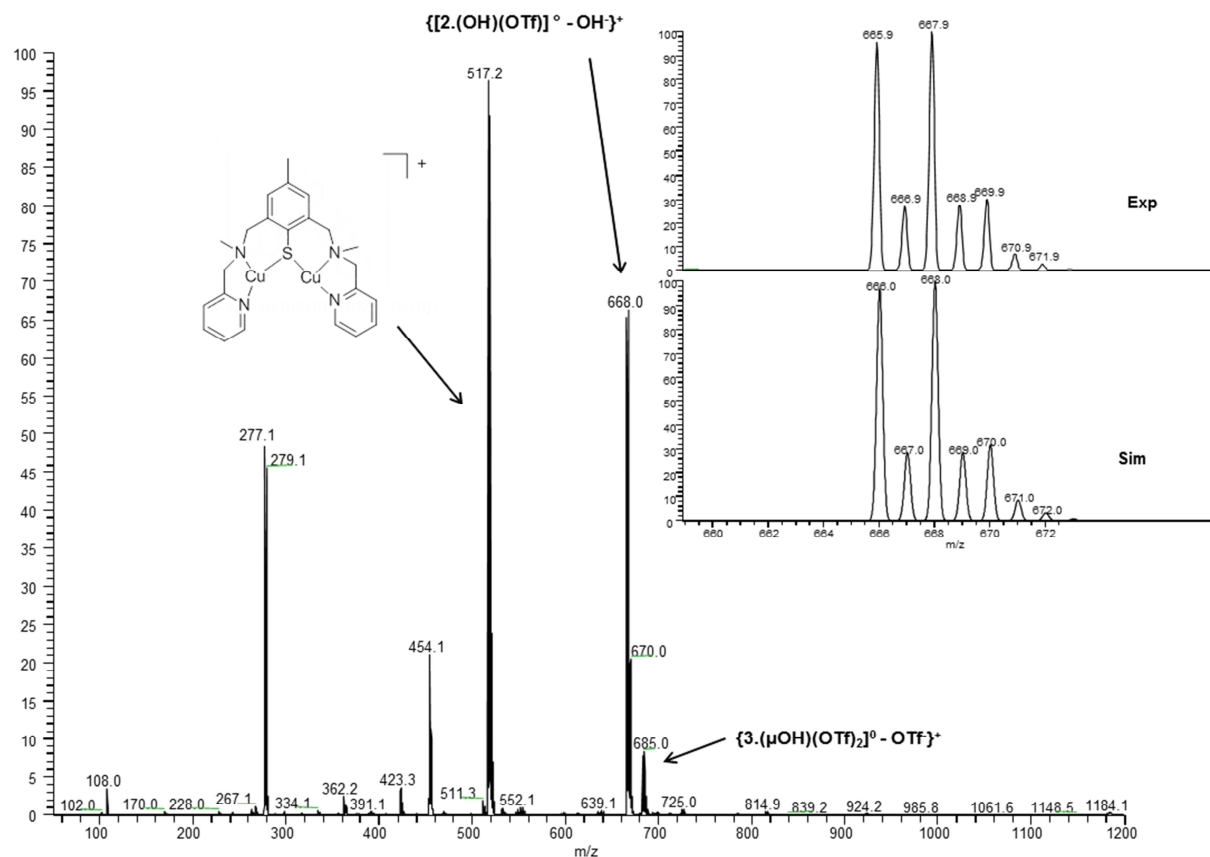


Figure S8. UV-Vis spectra of $[2.\text{(H}_2\text{O)}(\text{OTf})]^+$ (black), $[2.\text{(H}_2\text{O)}(\text{OTf})]^+ + 1.1$ molar equiv. of DABCO (green) and $[2.\text{(H}_2\text{O)}(\text{OTf})]^+ + 1.1$ molar equiv. of DABCO + O₂ (red);

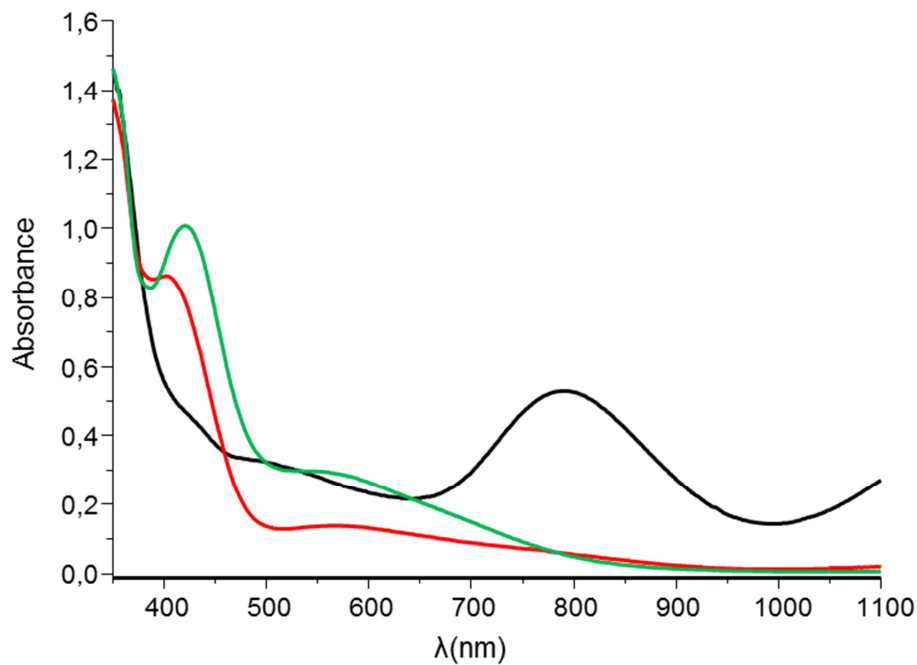


Figure S9. UV-Vis spectra for crystalline $[2.\text{(H}_2\text{O)}(\text{OTf})]^+$ in acetone before (dotted) and after addition of 200 molar equiv. NaOTf (solid).

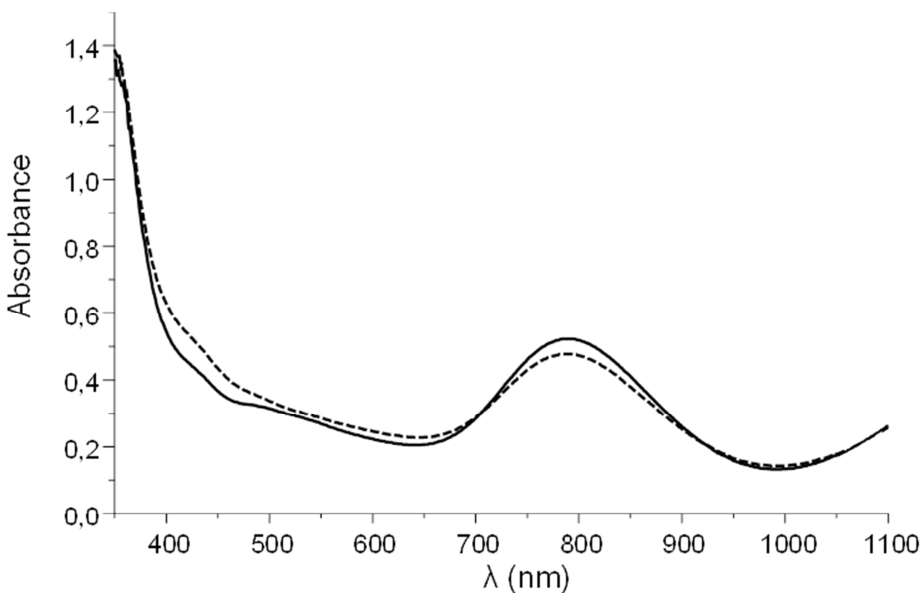


Figure S10. TD-DFT assignment of the calculated transitions for $[2.\text{(H}_2\text{O)}(\text{OTf})]^+$. The population of the relevant MOs (HOMO: Highest Occupied Molecular Orbital, LUMO: Lowest Unoccupied Molecular Orbital) is indicated in parenthesis as well as the wavelength of the optical transitions. S-Ph stands for the thiophenolate part of the ligand and L for the remaining part of the organic molecule.

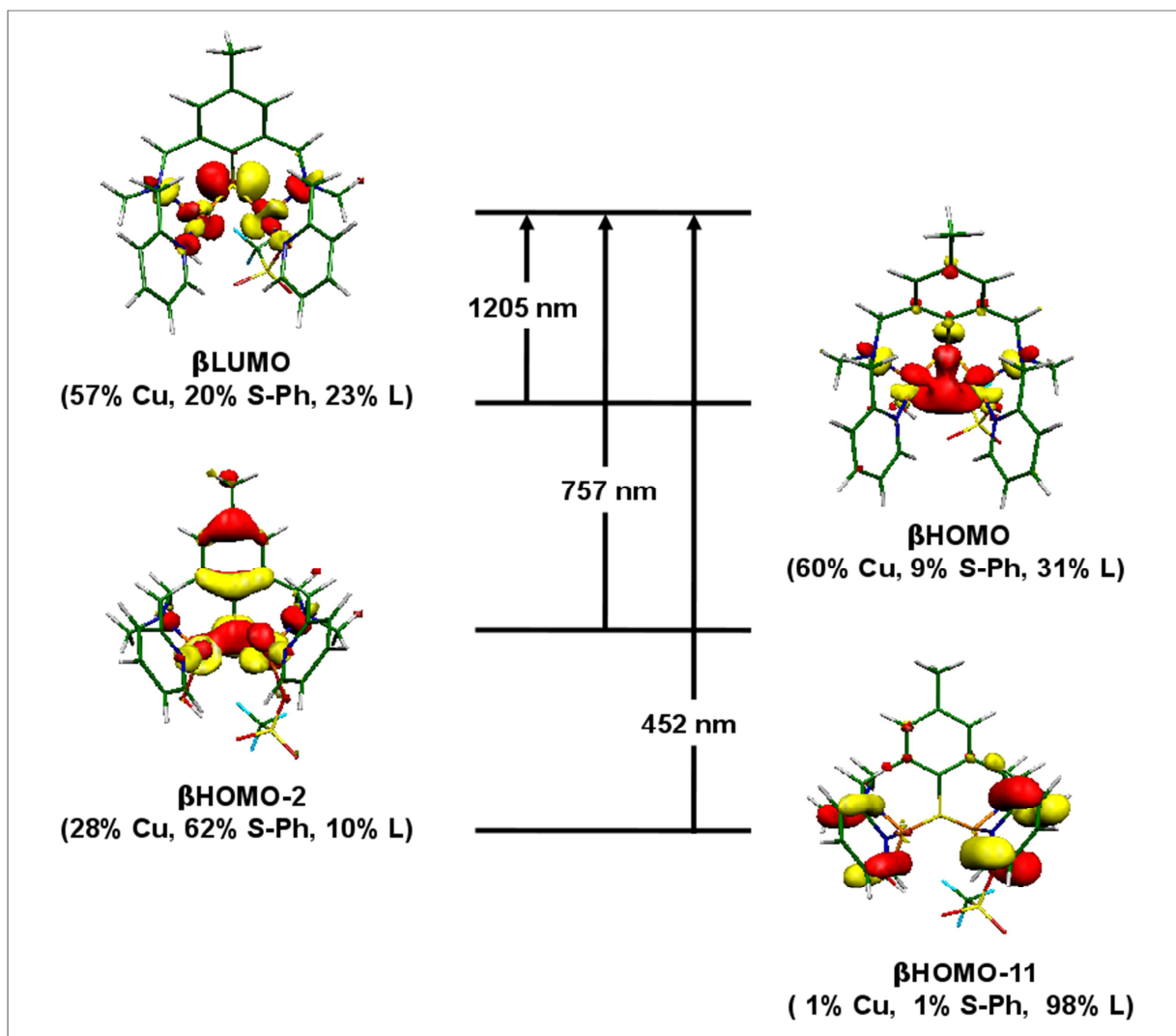


Figure S11. ^{19}F NMR spectra for triflates-containing standards used for our study.

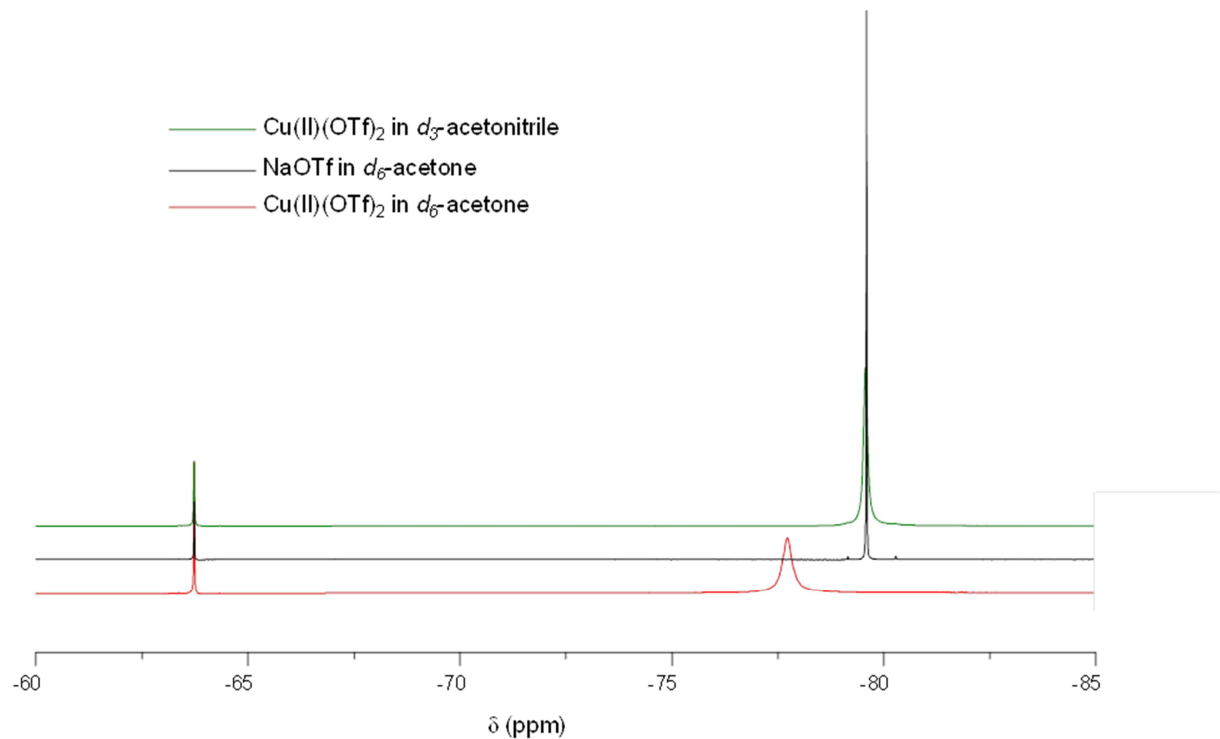


Figure S12. ^{19}F NMR shift variation of [1] and $[2.\text{(H}_2\text{O)(OTf)}]^+$ as a function of the temperature ($^{\circ}\text{C}$) in deuterated acetone.

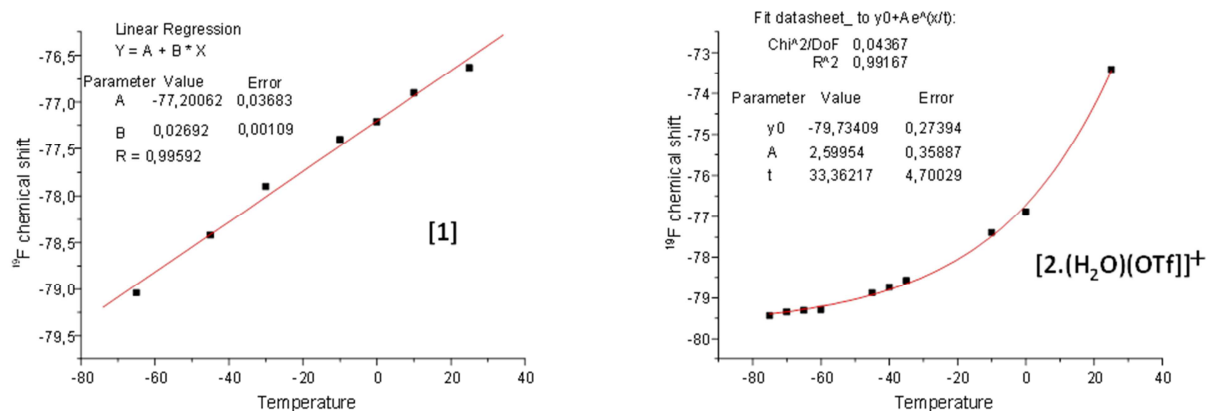


Figure S13. Cyclic voltammogram for a 3.20 mM solution of $[2.\text{(H}_2\text{O)(OTf)}]^+$ + 1.1 molar equiv. of DABCO in acetone + 0.1M $(\text{nBu})_4\text{NClO}_4$ vs. Ag/Ag(NO_3^-) (0.01 M in 0.1 M $(\text{nBu})_4\text{NClO}_4$). Glassy carbon disk as working electrode at 100 mV.s^{-1} .

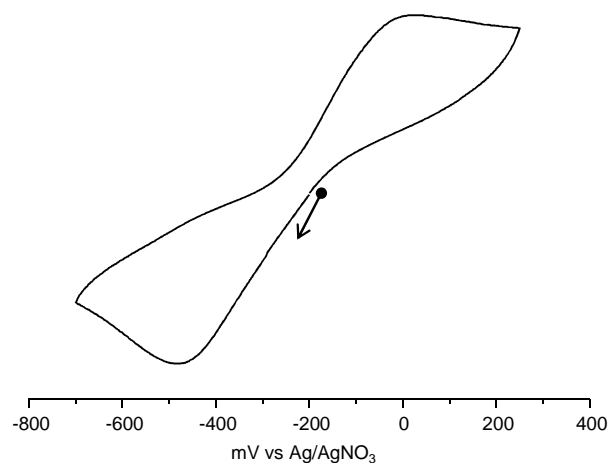


Figure S14. Cyclic voltammograms for a 1.54 mM solution of $[2.\text{(H}_2\text{O)(OTf)}]^+$ in acetone + 0.1M $(\text{nBu})_4\text{NClO}_4$ vs. Ag/Ag(NO_3^-) (0.01 M in 0.1 M $(\text{nBu})_4\text{NClO}_4$) without (A) and with (B) addition of excess NaOTf (200 molar equiv.). Glassy carbon disk as working electrode at 100 mV.s^{-1} .

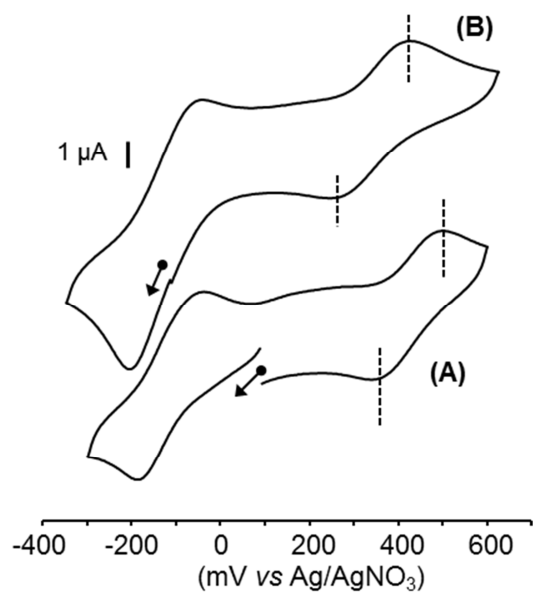


Figure S15. X-band EPR spectra of $[2.\text{(H}_2\text{O)}(\text{OTf})]^+$ (0.68 mM, solid) and $[2.\text{(H}_2\text{O)}(\text{OTf})]^+$ (0.68 mM) + 200 molar equiv. of NaOTf (dotted) in acetone at 10 K.

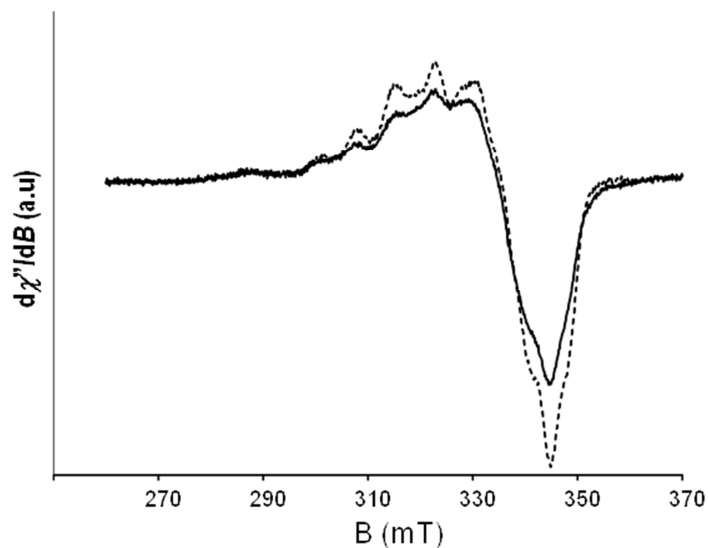


Figure S16. X-band EPR spectra of $[2.\text{(H}_2\text{O)}(\text{OTf})]^+ + 1.1$ molar equiv. of DABCO in acetone.

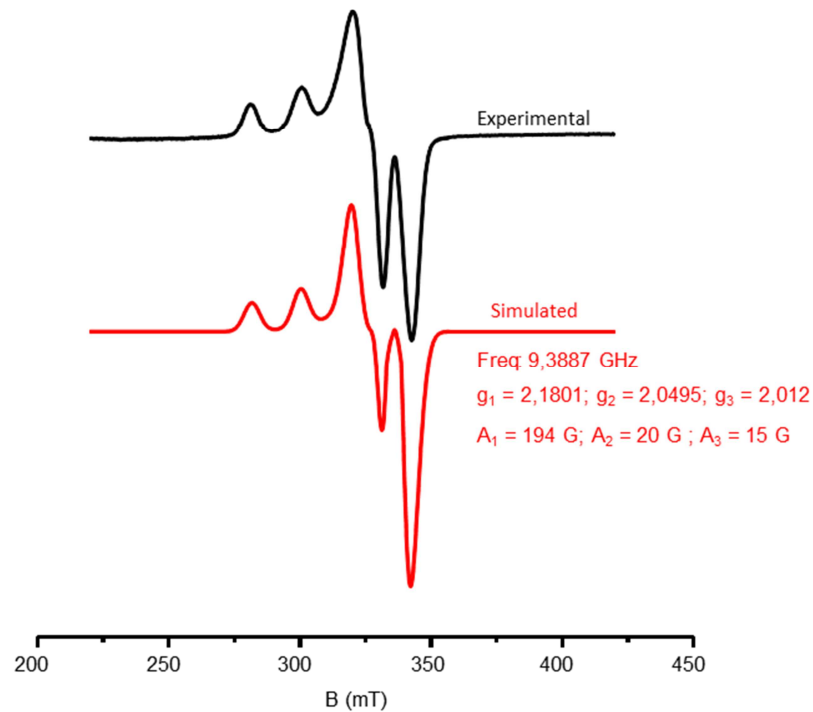


Figure S17. X-Band EPR evolution of $[2.\text{(H}_2\text{O)}(\text{OTf})]^+$ upon progressive N_2O -bubbling in acetone at 10K.

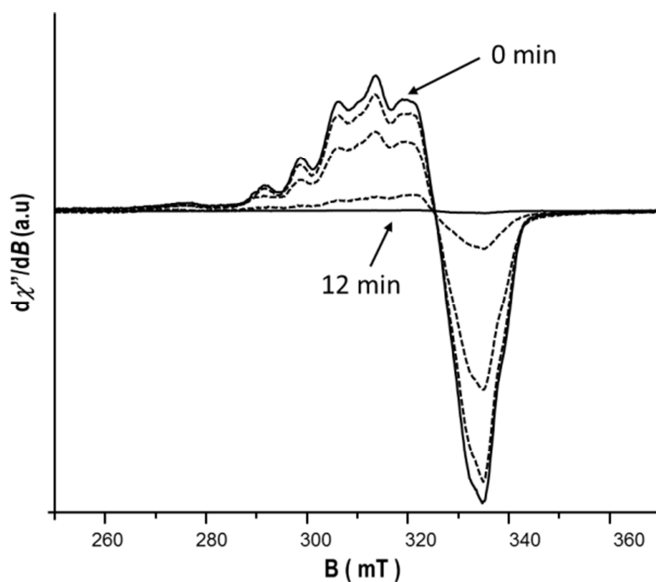


Figure S18. (A) Composition of the headspaces gas with a GC run of 0.6 min; (B) GC profile for the reaction of $[2.\text{(H}_2\text{O)}(\text{OTf})]^+$ (solid) and [1] (dotted) with N_2O showing the detection of N_2 at 0.5 min. The calculated N_2/O_2 ratio suggests that no O_2 contamination occurred during the experiment.

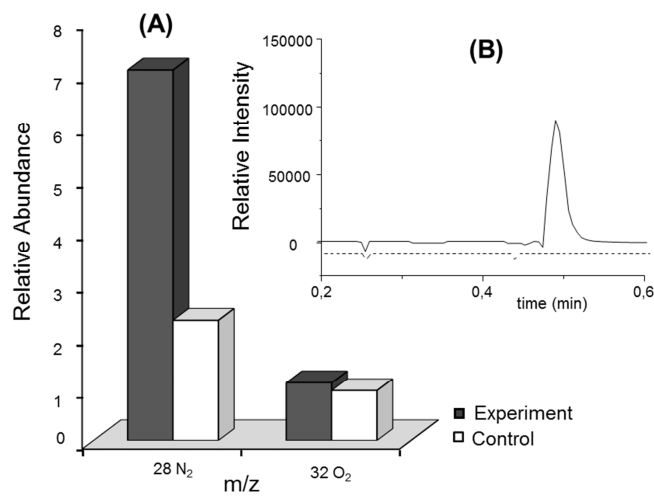


Figure S19. ESI mass spectrum of the bulk solution resulting from the reaction with N₂O in acetone; (Left) Experimental, (Right) Calculated for the corresponding hydroxo-containing product ([L^{MeMAMS}(OH)(OTf)]⁺ i.e [3.(μOH)(OTf)₂]).

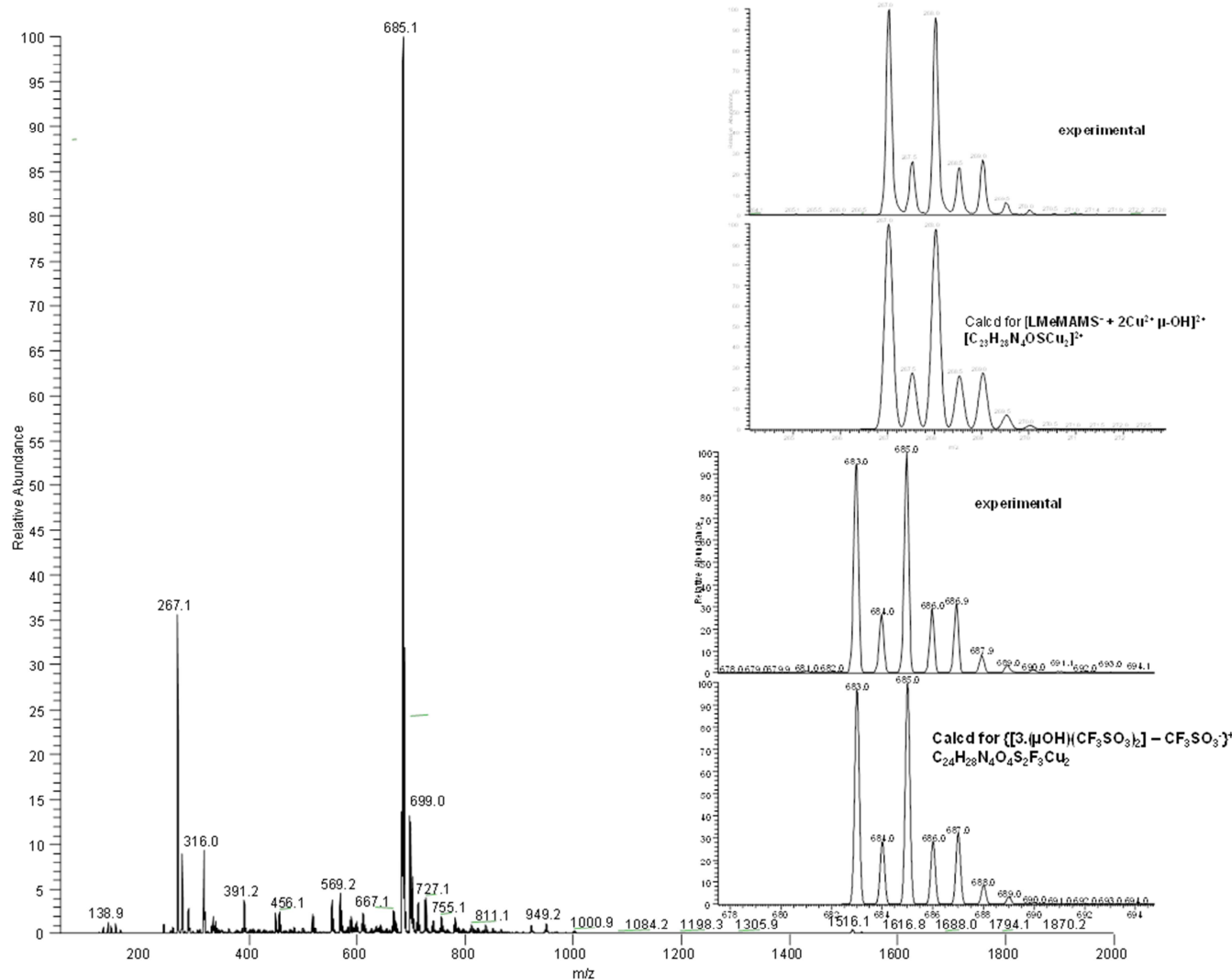
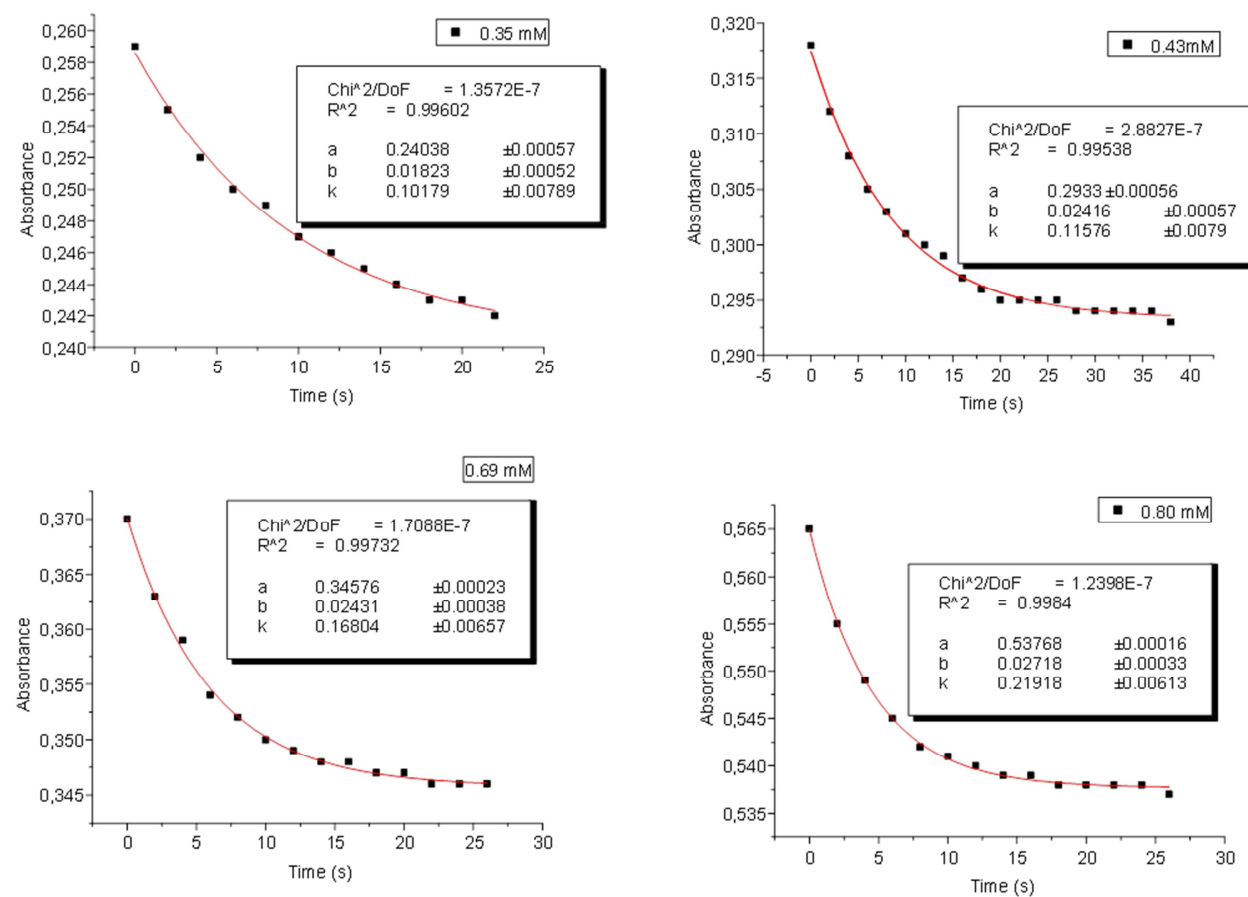


Figure S20. Determination of k' values according to various $[2.\text{(H}_2\text{O)}(\text{OTf})]^+$ concentrations upon monitoring the variation of absorbance at 787 nm.



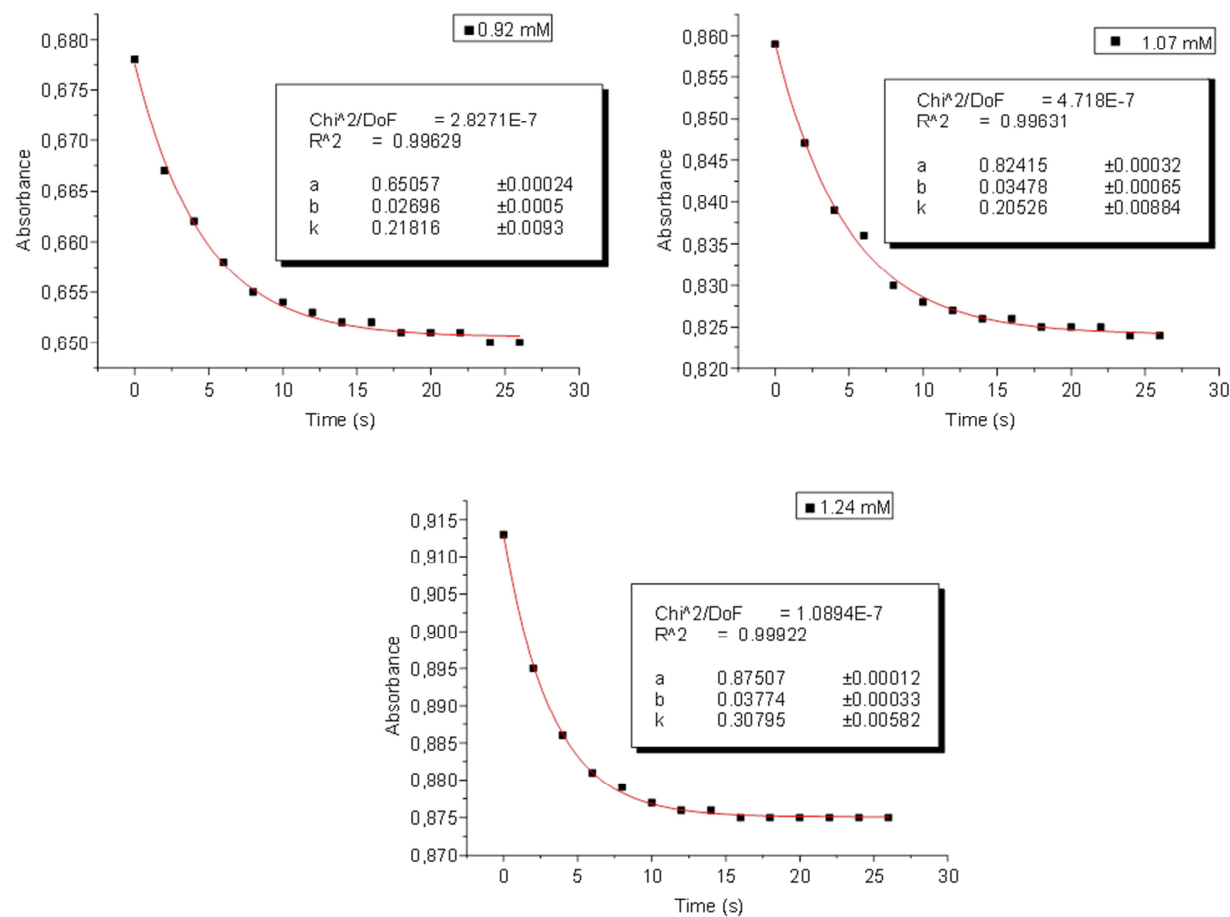


Figure S21. Plot of $\ln k'$ as a function of $[2\cdot(\text{H}_2\text{O})(\text{OTf})]^+$ concentration to determine the reaction *pseudo*-rate order.

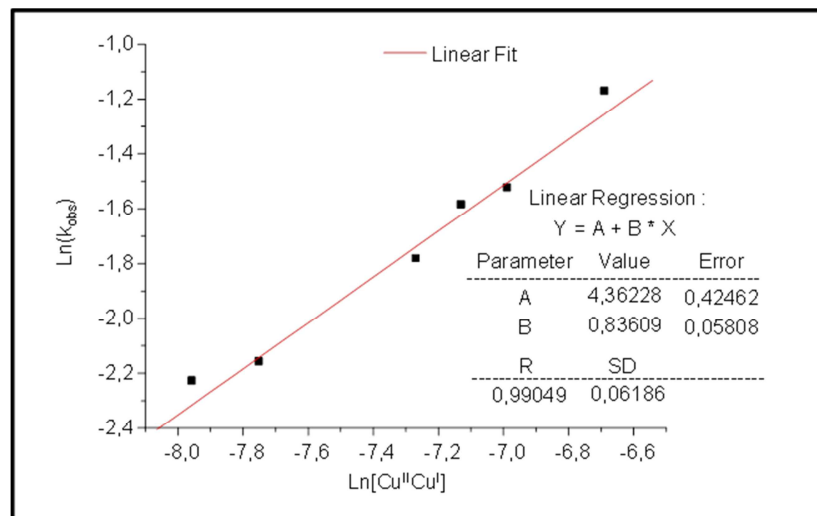


Figure S22. Evolution of the UV-Vis spectrum of $[2\cdot(\text{H}_2\text{O})(\text{OTf})]^+$ (black) upon successive addition of 1.1 molar equiv. of DABCO (green), N_2O bubbling (1 min (blue) and 2 min (pink)) and exposure to air (red).

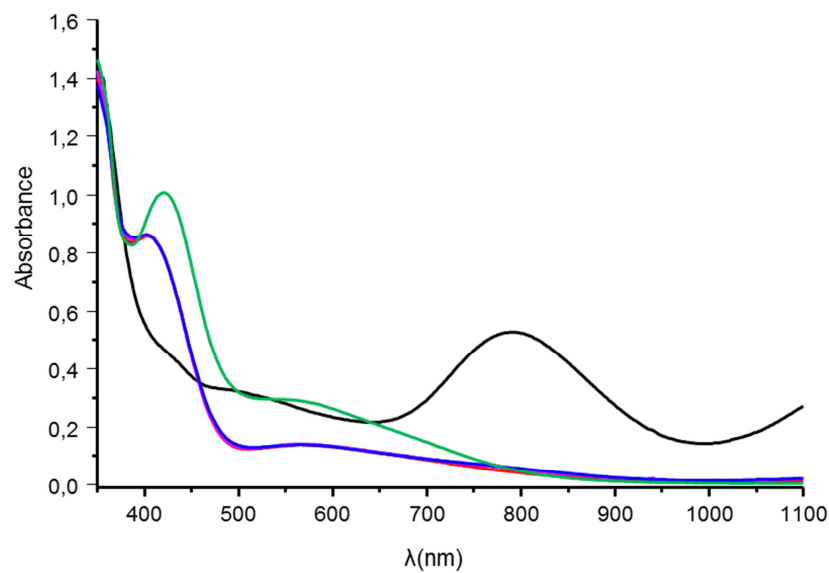


Figure S23. Calculated UV-Vis spectra for **(1)-(5)** and $[2.\text{(H}_2\text{O})(\text{OTf})]^+$.

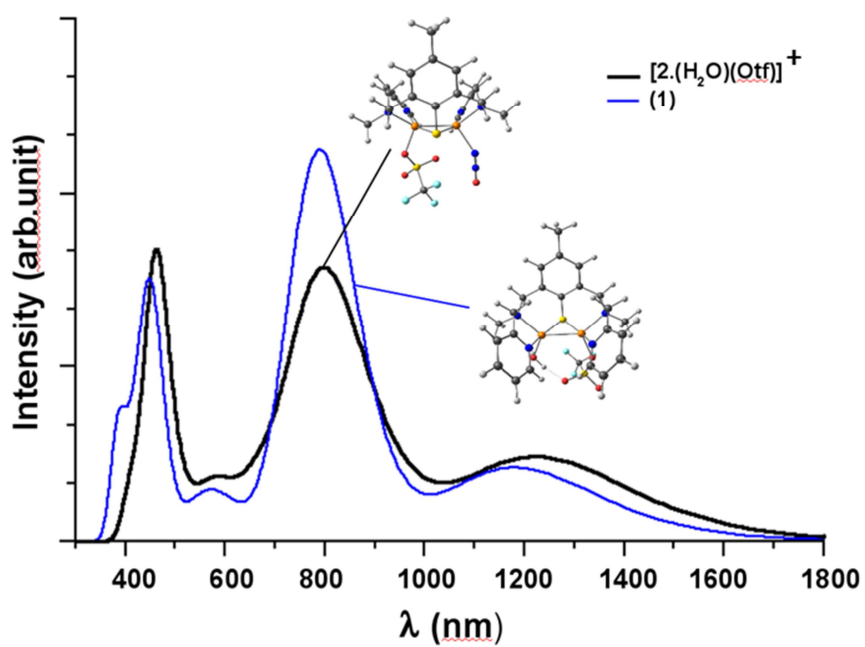
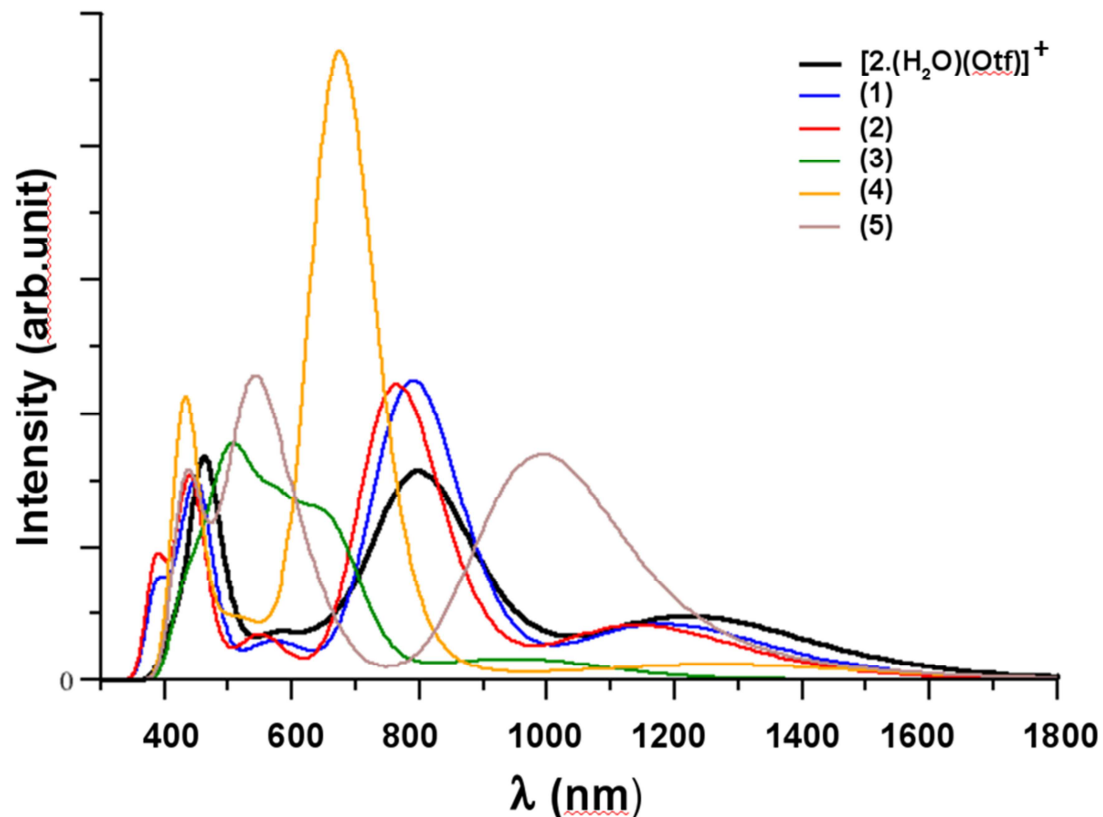


Figure S24. Spin-density plot (**a**) and localized SOMO (**b**) of (**1**).

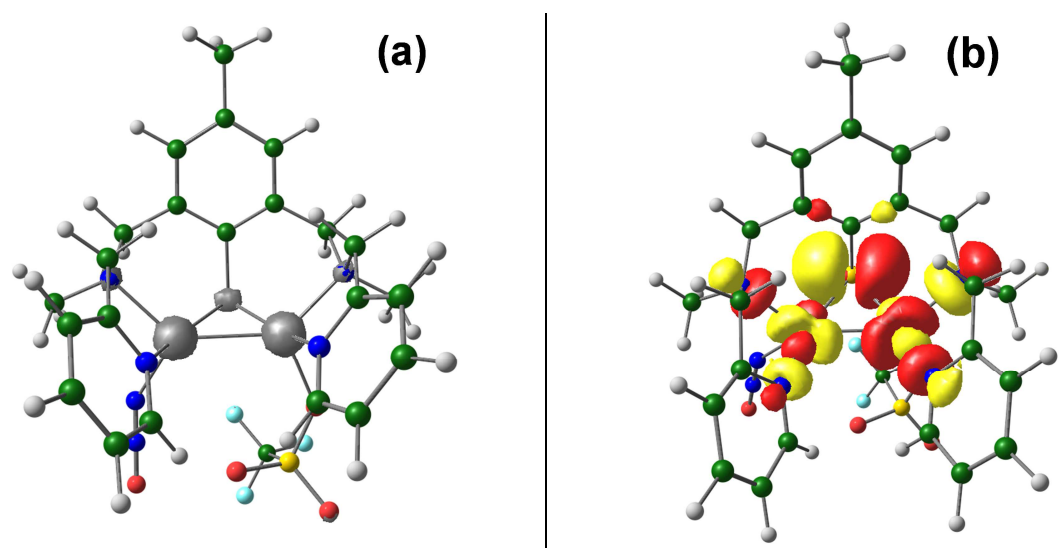


Table S1: Summary of X-Ray Crystallographic Data for **(C)**, **(D)**, **[2.(H₂O)(OTf)]⁺** and **[3.(μOH)(OTf)₂]**.

Compound	(D)	(C)	[2.(H ₂ O)(OTf)] ⁺	[3.(μOH)(OTf) ₂]
Empirical formula	C ₉ H ₉ Cl ₂ S	C ₁₉ H ₂₆ O ₅ S ₂	C ₂₅ H ₂₉ Cu ₂ F ₆ N ₄ O ₇ S ₃	C ₂₅ H ₂₈ Cu ₂ F ₆ N ₄ O ₇ S ₃
Formula Weight	220.12	398.52	834.78	833.77
Crystal System	Monoclinic	Triclinic	Triclinic	Triclinic
Space group	P 1 21/c 1	P -1	P -1	P -1
Unit Cell Dimensions	a = 16.8843(16) Å α = 90 ° b = 7.6695(4) Å β = 115.956(15)° c = 16.974(2) Å γ = 90 °	a = 8.5289(5) Å α= 87.759(5)° b = 10.9789(7) Å β = 72.017(5)° c = 11.4493(7) Å γ = 78.159(5)°	a = 9.8541(6) Å α = 93.504(6)° b = 11.4575(8) Å β = 98.701(6)° c = 15.9521(13) Å γ = 14.179(7)°	a = 9.6497(5) Å α = 73.733(4)° b = 10.7181(5) Å β = 86.706(4)° c = 16.8890(8) Å γ = 69.619(4)°
Volume, Z	1976.4(3) Å ³ , 8	997.68(11) Å ³ , 2	1608.9(2) Å ³ , 2	1570.30(13) Å ³ , 2
Density (calculated)	1.480 g/cm ³	1.327 g/cm ³	1.723 g/cm ³	1.763 g/cm ³
Absorption Coefficient	0.808 mm ⁻¹	0.293 mm ⁻¹	1.601 mm ⁻¹	1.640 mm ⁻¹
F(000)	904	424	846	844
Crystal Size	0.96 x 0.80 x 0.26 mm	0.26 x 0.21 x 0.10 mm	0.47 x 0.26 x 0.14 mm	0.25 x 0.18 x 0.11 mm
θ range for Data Collection	3.49 to 28.28 deg.	3.49 to 30.51 deg.	3.35 to 30.51 deg.	3.30 to 30.51 deg.
Limiting Indices	-22<=h<=22, -10<=k<=10, -22<=l<=20	-12<=h<=12, -15<=k<=10, -15<=l<=16	-14<=h<=14, -16<=k<=16, -22<=l<=22	-13<=h<=13, -15<=k<=15, -24<=l<=24
Reflections Collected	9370	9120	19709	19076
Independent Reflections	4674 [R(int) = 0.0277]	6009 [R(int) = 0.0284]	9796 [R(int) = 0.0237]	9486 [R(int) = 0.0522]
Max and Min Transmission	0.8167 and 0.5099	0.9724 and 0.9283	0.8023 and 0.5194	0.8351 and 0.6846
Data/Restains/Parameters	4674 / 0 / 289	6009 / 0 / 340	9796 / 0 / 540	9486 / 0 / 427
Goodness-of-fit on F ²	1.071	0.802	1.035	0.993
Final R Indices [I>2σ(I)]	R1 = 0.0429, wR2 = 0.0924	R1 = 0.0429, wR2 = 0.0720	R1 = 0.0356, wR2 = 0.0783	R1 = 0.0580, wR2 = 0.0952
R Indices (all data)	R1 = 0.0591, wR2 = 0.1012	R1 = 0.0810, wR2 = 0.0768	R1 = 0.0503, wR2 = 0.0849	R1 = 0.1164, wR2 = 0.1123

Table S2. Bond lengths [Å] and angles [deg] for (**C**).

S(1)-C(1)	1.7796(16)	C(19)-H(19B)	0.991(19)	C(16)-C(11)-C(12)	120.13(17)
S(1)-S(2)	2.0717(6)	O(21)-C(21)	1.405(3)	C(16)-C(11)-S(2)	120.57(12)
O(1)-C(7)	1.4217(19)	O(21)-H(21O)	0.90(3)	C(12)-C(11)-S(2)	119.29(12)
O(1)-H(1O)	0.81(2)	C(21)-H(21A)	0.89(2)	C(13)-C(12)-C(11)	118.48(15)
O(2)-C(9)	1.434(2)	C(21)-H(21B)	0.96(3)	C(13)-C(12)-C(17)	118.81(16)
O(2)-H(2O)	0.78(2)	C(21)-H(21C)	0.94(2)	C(11)-C(12)-C(17)	122.66(18)
C(1)-C(6)	1.399(2)	C(1)-S(1)-S(2)	103.31(5)	C(12)-C(13)-C(14)	122.68(17)
C(1)-C(2)	1.407(2)	C(7)-O(1)-H(1O)	111.4(16)	C(12)-C(13)-H(13)	118.3(11)
C(2)-C(3)	1.388(2)	C(9)-O(2)-H(2O)	106.8(15)	C(14)-C(13)-H(13)	119.0(11)
C(2)-C(7)	1.510(2)	C(6)-C(1)-C(2)	120.63(14)	C(13)-C(14)-C(15)	117.31(19)
C(3)-C(4)	1.388(2)	C(6)-C(1)-S(1)	118.76(11)	C(13)-C(14)-C(18)	121.32(19)
C(3)-H(3)	0.951(15)	C(2)-C(1)-S(1)	120.57(13)	C(15)-C(14)-C(18)	121.36(19)
C(4)-C(5)	1.388(2)	C(3)-C(2)-C(1)	118.22(16)	C(16)-C(15)-C(14)	122.60(17)
C(4)-C(8)	1.506(3)	C(3)-C(2)-C(7)	121.36(14)	C(16)-C(15)-H(15)	120.8(11)
C(5)-C(6)	1.393(2)	C(1)-C(2)-C(7)	120.42(14)	C(14)-C(15)-H(15)	116.6(11)
C(5)-H(5)	0.970(18)	C(4)-C(3)-C(2)	122.29(15)	C(15)-C(16)-C(11)	118.74(15)
C(6)-C(9)	1.509(2)	C(4)-C(3)-H(3)	119.9(10)	C(15)-C(16)-C(19)	120.68(15)
C(7)-H(7A)	0.958(16)	C(2)-C(3)-H(3)	117.8(10)	C(11)-C(16)-C(19)	120.57(17)
C(7)-H(7B)	0.982(16)	C(5)-C(4)-C(3)	118.39(15)	O(11)-C(17)-C(12)	112.77(14)
C(8)-H(8A)	0.93(3)	C(5)-C(4)-C(8)	120.08(18)	O(11)-C(17)-H(17A)	108.4(10)
C(8)-H(8B)	0.87(3)	C(3)-C(4)-C(8)	121.53(17)	C(12)-C(17)-H(17A)	111.6(9)
C(8)-H(8C)	0.86(2)	C(4)-C(5)-C(6)	121.53(17)	O(11)-C(17)-H(17B)	105.9(11)
C(9)-H(9A)	1.00(2)	C(4)-C(5)-H(5)	119.7(10)	C(12)-C(17)-H(17B)	109.7(12)
C(9)-H(9B)	0.998(18)	C(6)-C(5)-H(5)	118.7(10)	H(17A)-C(17)-H(17B)	108.2(15)
S(2)-C(11)	1.7751(18)	C(5)-C(6)-C(1)	118.93(15)	C(14)-C(18)-H(18A)	113.2(15)
O(11)-C(17)	1.417(2)	C(5)-C(6)-C(9)	118.35(16)	C(14)-C(18)-H(18B)	113.7(19)
O(11)-H(11O)	0.77(2)	C(1)-C(6)-C(9)	122.65(15)	H(18A)-C(18)-H(18B)	105(2)
O(12)-C(19)	1.422(2)	O(1)-C(7)-C(2)	113.83(14)	C(14)-C(18)-H(18C)	109(2)
O(12)-H(12O)	0.777(19)	O(1)-C(7)-H(7A)	105.8(10)	H(18A)-C(18)-H(18C)	106(2)
C(11)-C(16)	1.405(2)	C(2)-C(7)-H(7A)	108.1(10)	H(18B)-C(18)-H(18C)	110(3)
C(11)-C(12)	1.405(2)	O(1)-C(7)-H(7B)	111.0(9)	O(12)-C(19)-C(16)	112.42(17)
C(12)-C(13)	1.384(3)	C(2)-C(7)-H(7B)	109.3(10)	O(12)-C(19)-H(19A)	107.3(9)
C(12)-C(17)	1.504(2)	H(7A)-C(7)-H(7B)	108.7(13)	C(16)-C(19)-H(19A)	110.0(9)
C(13)-C(14)	1.389(2)	C(4)-C(8)-H(8A)	109.8(18)	O(12)-C(19)-H(19B)	109.0(10)
C(13)-H(13)	0.950(16)	C(4)-C(8)-H(8B)	111.4(19)	C(16)-C(19)-H(19B)	109.8(10)
C(14)-C(15)	1.389(3)	H(8A)-C(8)-H(8B)	106(2)	H(19A)-C(19)-H(19B)	108.1(15)
C(14)-C(18)	1.501(3)	C(4)-C(8)-H(8C)	113.5(17)	O(21)-C(21)-H(21A)	107.7(16)
C(15)-C(16)	1.380(3)	H(8A)-C(8)-H(8C)	107(2)	O(21)-C(21)-H(21B)	111.2(17)
C(15)-H(15)	0.926(15)	H(8B)-C(8)-H(8C)	108(2)	H(21A)-C(21)-H(21B)	101(2)
C(16)-C(19)	1.512(2)	O(2)-C(9)-C(6)	111.92(15)	O(21)-C(21)-H(21C)	110.5(15)
C(17)-H(17A)	0.992(18)	O(2)-C(9)-H(9A)	109.2(9)	H(21A)-C(21)-H(21C)	117(2)
C(17)-H(17B)	0.96(2)	C(6)-C(9)-H(9A)	110.1(9)	H(21B)-C(21)-H(21C)	109(2)
C(18)-H(18A)	0.91(2)	O(2)-C(9)-H(9B)	107.0(10)		
C(18)-H(18B)	0.97(3)	C(6)-C(9)-H(9B)	112.4(10)		
C(18)-H(18C)	0.94(3)	H(9A)-C(9)-H(9B)	106.1(15)		
C(19)-H(19A)	0.984(18)	C(11)-S(2)-S(1)	101.84(5)		
		C(17)-O(11)-H(11O)	111.5(16)		
		C(19)-O(12)-H(12O)	109.9(15)		

Hydrogen bonds for (**C**) [Å and deg.].

D-H...A	d(D-H)	d(H...A)	d(D...A)	<(DHA)	Symmetry transformations used to generate equivalent atoms:
O(21)-H(21O)...O(2)	0.90(3)	1.85(3)	2.709(2)	158(2)	#1 -x+1,-y,-z
O(11)-H(11O)...O(12)#1	0.77(2)	1.90(2)	2.6615(18)	171(2)	#2 -x+1,-y,-z+1
O(12)-H(12O)...O(21)#2	0.777(19)	1.878(19)	2.6520(19)	174(2)	#3 -x,y+1,-z+1
O(2)-H(2O)...O(1)#3	0.78(2)	2.00(2)	2.7649(18)	170(2)	#4 -x,y+1,-z
O(1)-H(1O)...O(11)#4	0.81(2)	1.88(2)	2.6895(18)	176(2)	

Table S3. Bond lengths [Å] and angles [deg] for (**D**).

S(1)-C(1)	1.780(2)	C(1)-S(1)-S(2)	101.68(8)	C(14)-C(13)-H(13)	118.8(16)
S(1)-S(2)	2.0668(9)	C(11)-S(2)-S(1)	103.18(7)	C(12)-C(13)-H(13)	119.3(16)
S(2)-C(11)	1.783(2)	C(2)-C(1)-C(6)	119.7(2)	C(15)-C(14)-C(13)	118.3(2)
Cl(1)-C(7)	1.812(3)	C(2)-C(1)-S(1)	120.47(18)	C(15)-C(14)-C(19)	121.3(2)
Cl(2)-C(8)	1.794(2)	C(6)-C(1)-S(1)	119.80(17)	C(13)-C(14)-C(19)	120.4(2)
Cl(11)-C(17)	1.778(3)	C(3)-C(2)-C(1)	119.2(2)	C(14)-C(15)-C(16)	122.2(2)
Cl(12)-C(18)	1.803(3)	C(3)-C(2)-C(7)	118.8(2)	C(14)-C(15)-H(15)	117.7(19)
C(1)-C(2)	1.408(3)	C(1)-C(2)-C(7)	122.0(2)	C(16)-C(15)-H(15)	120.1(19)
C(1)-C(6)	1.409(3)	C(2)-C(3)-C(4)	122.1(2)	C(15)-C(16)-C(11)	118.6(2)
C(2)-C(3)	1.392(3)	C(2)-C(3)-H(3)	118.6(15)	C(15)-C(16)-C(18)	117.9(2)
C(2)-C(7)	1.494(3)	C(4)-C(3)-H(3)	119.2(16)	C(11)-C(16)-C(18)	123.5(2)
C(3)-C(4)	1.394(4)	C(5)-C(4)-C(3)	117.8(2)	C(12)-C(17)-Cl(11)	111.34(17)
C(3)-H(3)	0.92(2)	C(5)-C(4)-C(9)	120.9(3)	C(12)-C(17)-H(17A)	111(2)
C(4)-C(5)	1.391(3)	C(3)-C(4)-C(9)	121.3(3)	Cl(11)-C(17)-H(17A)	106.7(19)
C(4)-C(9)	1.507(4)	C(4)-C(5)-C(6)	122.3(2)	C(12)-C(17)-H(17B)	109(2)
C(5)-C(6)	1.394(4)	C(4)-C(5)-H(5)	119.2(17)	Cl(11)-C(17)-H(17B)	108(2)
C(5)-H(5)	0.97(3)	C(6)-C(5)-H(5)	118.5(17)	H(17A)-C(17)-H(17B)	110(3)
C(6)-C(8)	1.498(3)	C(5)-C(6)-C(1)	119.0(2)	C(16)-C(18)-Cl(12)	110.75(18)
C(7)-H(7A)	0.97(3)	C(5)-C(6)-C(8)	118.6(2)	C(16)-C(18)-H(18A)	113.0(17)
C(7)-H(7B)	0.97(3)	C(1)-C(6)-C(8)	122.4(2)	Cl(12)-C(18)-H(18A)	103.6(16)
C(8)-H(8A)	0.95(3)	C(2)-C(7)-Cl(1)	111.29(17)	C(16)-C(18)-H(18B)	112.4(18)
C(8)-H(8B)	0.93(3)	C(2)-C(7)-H(7A)	110.3(19)	Cl(12)-C(18)-H(18B)	107.0(17)
C(9)-H(9A)	0.91(5)	Cl(1)-C(7)-H(7A)	105.9(19)	H(18A)-C(18)-H(18B)	110(2)
C(9)-H(9B)	0.85(5)	C(2)-C(7)-H(7B)	113.4(16)	C(14)-C(19)-H(19A)	112(3)
C(9)-H(9C)	0.91(6)	Cl(1)-C(7)-H(7B)	106.7(17)	C(14)-C(19)-H(19B)	117(4)
C(11)-C(12)	1.403(3)	H(7A)-C(7)-H(7B)	109(2)	H(19A)-C(19)-H(19B)	111(4)
C(11)-C(16)	1.408(3)	C(6)-C(8)-Cl(2)	110.16(16)	C(14)-C(19)-H(19C)	114(3)
C(12)-C(13)	1.396(3)	C(6)-C(8)-H(8A)	115.2(17)	H(19A)-C(19)-H(19C)	102(4)
C(12)-C(17)	1.503(3)	Cl(2)-C(8)-H(8A)	107.1(17)	H(19B)-C(19)-H(19C)	99(4)
C(13)-C(14)	1.389(3)	C(6)-C(8)-H(8B)	109.3(18)		
C(13)-H(13)	0.93(3)	Cl(2)-C(8)-H(8B)	106.5(17)		
C(14)-C(15)	1.380(3)	H(8A)-C(8)-H(8B)	108(2)		
C(14)-C(19)	1.504(4)	C(4)-C(9)-H(9A)	110(3)		
C(15)-C(16)	1.398(3)	C(4)-C(9)-H(9B)	117(4)		
C(15)-H(15)	0.91(3)	H(9A)-C(9)-H(9B)	101(4)		
C(16)-C(18)	1.490(3)	C(4)-C(9)-H(9C)	114(3)		
C(17)-H(17A)	0.92(3)	H(9A)-C(9)-H(9C)	111(4)		
C(17)-H(17B)	0.92(4)	H(9B)-C(9)-H(9C)	104(4)		
C(18)-H(18A)	0.93(3)	C(12)-C(11)-C(16)	120.0(2)		
C(18)-H(18B)	0.91(3)	C(12)-C(11)-S(2)	119.94(17)		
C(19)-H(19A)	0.91(5)	C(16)-C(11)-S(2)	120.04(18)		
C(19)-H(19B)	0.82(6)	C(13)-C(12)-C(11)	119.0(2)		
C(19)-H(19C)	0.85(5)	C(13)-C(12)-C(17)	117.8(2)		
		C(11)-C(12)-C(17)	123.3(2)		
		C(14)-C(13)-C(12)	121.8(2)		

Table S4. Bond lengths [Å] and angles [deg] for **[2.(H₂O)(OTf)]⁺**.

Cu(1)-N(3)	1.9744(16)	C(16)-H(16B)	0.99(3)	Cu(1)-O(1)-H(1O)	124(2)
Cu(1)-N(1)	2.0627(16)	C(17)-C(18)	1.386(3)	Cu(1)-O(1)-H(2O)	110(2)
Cu(1)-O(1)	2.1643(17)	C(18)-C(19)	1.389(3)	H(1O)-O(1)-H(2O)	105(3)
Cu(1)-S(1)	2.1806(5)	C(18)-H(18)	0.94(3)	C(22)-N(1)-C(10)	110.76(16)
Cu(1)-Cu(2)	2.5674(4)	C(19)-C(20)	1.383(4)	C(22)-N(1)-C(7)	108.56(16)
Cu(2)-N(4)	1.9562(17)	C(19)-H(19)	0.96(3)	C(10)-N(1)-C(7)	111.39(16)
Cu(2)-N(2)	2.0737(16)	C(20)-C(21)	1.377(3)	C(22)-N(1)-Cu(1)	108.40(13)
Cu(2)-S(1)	2.1686(5)	C(20)-H(20)	0.86(3)	C(10)-N(1)-Cu(1)	104.09(12)
Cu(2)-O(1S2)	2.2115(15)	C(21)-H(21)	0.96(2)	C(7)-N(1)-Cu(1)	113.58(11)
S(1)-C(1)	1.800(2)	C(22)-H(22A)	0.98(2)	C(16)-N(2)-C(23)	110.11(16)
O(1)-H(1O)	0.80(3)	C(22)-H(22B)	0.90(3)	C(16)-N(2)-C(8)	111.94(17)
O(1)-H(2O)	0.68(3)	C(22)-H(22C)	0.93(2)	C(23)-N(2)-C(8)	108.00(16)
N(1)-C(22)	1.473(3)	C(23)-H(23A)	0.98(2)	C(16)-N(2)-Cu(2)	101.55(12)
N(1)-C(10)	1.483(3)	C(23)-H(23B)	0.90(3)	C(23)-N(2)-Cu(2)	111.90(13)
N(1)-C(7)	1.490(2)	C(23)-H(23C)	0.93(3)	C(8)-N(2)-Cu(2)	113.28(12)
N(2)-C(16)	1.481(3)	S(2)-O(3S2)	1.4330(16)	C(15)-N(3)-C(11)	118.64(17)
N(2)-C(23)	1.483(3)	S(2)-O(2S2)	1.4451(17)	C(15)-N(3)-Cu(1)	128.08(14)
N(2)-C(8)	1.483(3)	S(2)-O(1S2)	1.4456(16)	C(11)-N(3)-Cu(1)	113.13(13)
N(3)-C(15)	1.342(3)	S(2)-C(2S)	1.819(3)	C(17)-N(4)-C(21)	118.95(18)
N(3)-C(11)	1.353(3)	F(1S2)-C(2S)	1.336(3)	C(17)-N(4)-Cu(2)	112.00(13)
N(4)-C(17)	1.346(3)	F(2S2)-C(2S)	1.326(3)	C(21)-N(4)-Cu(2)	128.38(15)
N(4)-C(21)	1.348(3)	F(3S2)-C(2S)	1.322(3)	C(6)-C(1)-C(2)	120.00(18)
C(1)-C(6)	1.403(3)	S(3)-O(2S3)	1.423(2)	C(6)-C(1)-S(1)	120.41(14)
C(1)-C(2)	1.404(3)	S(3)-O(3S3)	1.435(2)	C(2)-C(1)-S(1)	119.57(15)
C(2)-C(3)	1.395(3)	S(3)-O(1S3)	1.4499(18)	C(3)-C(2)-C(1)	119.41(18)
C(2)-C(7)	1.504(3)	S(3)-C(3S)	1.818(3)	C(3)-C(2)-C(7)	119.14(17)
C(3)-C(4)	1.393(3)	F(1S3)-C(3S)	1.324(3)	C(1)-C(2)-C(7)	121.42(18)
C(3)-H(3)	0.93(2)	F(2S3)-C(3S)	1.348(3)	C(4)-C(3)-C(2)	121.66(19)
C(4)-C(5)	1.393(3)	F(3S3)-C(3S)	1.336(3)	C(4)-C(3)-H(3)	119.3(15)
C(4)-C(9)	1.506(3)	N(3)-Cu(1)-N(1)	83.54(6)	C(2)-C(3)-H(3)	119.0(15)
C(5)-C(6)	1.391(3)	N(3)-Cu(1)-O(1)	92.49(7)	C(5)-C(4)-C(3)	117.56(19)
C(5)-H(5)	0.93(3)	N(1)-Cu(1)-O(1)	109.35(7)	C(5)-C(4)-C(9)	121.3(2)
C(6)-C(8)	1.515(3)	N(3)-Cu(1)-S(1)	156.55(5)	C(3)-C(4)-C(9)	121.1(2)
C(7)-H(7A)	0.97(2)	N(1)-Cu(1)-S(1)	98.51(5)	C(6)-C(5)-C(4)	122.7(2)
C(7)-H(7B)	0.92(2)	O(1)-Cu(1)-S(1)	108.57(5)	C(6)-C(5)-H(5)	119.2(16)
C(8)-H(8A)	0.93(3)	N(3)-Cu(1)-Cu(2)	110.63(5)	C(4)-C(5)-H(5)	118.1(16)
C(8)-H(8B)	0.99(2)	N(1)-Cu(1)-Cu(2)	138.77(5)	C(5)-C(6)-C(1)	118.59(18)
C(9)-H(9A)	0.93(3)	O(1)-Cu(1)-Cu(2)	108.46(5)	C(5)-C(6)-C(8)	119.22(18)
C(9)-H(9B)	0.92(4)	S(1)-Cu(1)-Cu(2)	53.604(15)	C(1)-C(6)-C(8)	122.05(18)
C(9)-H(9C)	0.95(4)	N(4)-Cu(2)-N(2)	84.81(7)	N(1)-C(7)-C(2)	112.51(15)
C(10)-C(11)	1.503(3)	N(4)-Cu(2)-S(1)	159.31(5)	N(1)-C(7)-H(7A)	106.5(14)
C(10)-H(10A)	0.97(2)	N(2)-Cu(2)-S(1)	99.61(5)	C(2)-C(7)-H(7A)	111.2(13)
C(10)-H(10B)	0.97(2)	N(4)-Cu(2)-O(1S2)	92.51(7)	N(1)-C(7)-H(7B)	109.1(14)
C(11)-C(12)	1.380(3)	N(2)-Cu(2)-O(1S2)	103.17(6)	C(2)-C(7)-H(7B)	108.6(14)
C(12)-C(13)	1.386(3)	S(1)-Cu(2)-O(1S2)	105.95(5)	H(7A)-C(7)-H(7B)	108.9(18)
C(12)-H(12)	0.93(3)	N(4)-Cu(2)-Cu(1)	109.85(5)	N(2)-C(8)-C(6)	114.67(16)
C(13)-C(14)	1.377(3)	N(2)-Cu(2)-Cu(1)	137.82(5)	N(2)-C(8)-H(8A)	110.3(15)
C(13)-H(13)	0.91(3)	S(1)-Cu(2)-Cu(1)	54.038(15)	C(6)-C(8)-H(8A)	107.0(15)
C(14)-C(15)	1.380(3)	O(1S2)-Cu(2)-Cu(1)	114.93(4)	N(2)-C(8)-H(8B)	107.2(13)
C(14)-H(14)	0.89(3)	C(1)-S(1)-Cu(2)	97.40(6)	C(6)-C(8)-H(8B)	109.3(12)
C(15)-H(15)	0.94(2)	C(1)-S(1)-Cu(1)	95.90(6)	H(8A)-C(8)-H(8B)	108(2)
C(16)-C(17)	1.511(3)	Cu(2)-S(1)-Cu(1)	72.358(17)	C(4)-C(9)-H(9A)	111.0(19)
C(16)-H(16A)	0.98(2)	H(23A)-C(23)-H(23C)	111(2)		
H(9A)-C(9)-H(9B)	105(3)	H(23B)-C(23)-H(23C)	110(2)		
C(4)-C(9)-H(9C)	115(2)	O(3S2)-S(2)-O(2S2)	115.53(10)		
H(9A)-C(9)-H(9C)	107(3)	O(3S2)-S(2)-O(1S2)	114.41(10)		
N(1)-C(10)-C(11)	109.96(16)	O(2S2)-S(2)-O(1S2)	114.49(10)		
N(1)-C(10)-H(10A)	110.4(14)	O(3S2)-S(2)-C(2S)	103.65(11)		
C(11)-C(10)-H(10A)	107.0(14)	O(2S2)-S(2)-C(2S)	103.47(11)		
N(1)-C(10)-H(10B)	112.6(14)	O(1S2)-S(2)-C(2S)	103.03(11)		

C(11)-C(10)-H(10B)	110.0(15)	F(3S2)-C(2S)-F(2S2)	107.6(2)
H(10A)-C(10)-H(10B)	107(2)	F(3S2)-C(2S)-F(1S2)	108.1(2)
N(3)-C(11)-C(12)	121.81(19)	F(2S2)-C(2S)-F(1S2)	107.9(2)
N(3)-C(11)-C(10)	115.57(17)	F(3S2)-C(2S)-S(2)	111.08(18)
C(12)-C(11)-C(10)	122.58(19)	F(2S2)-C(2S)-S(2)	110.83(19)
C(11)-C(12)-C(13)	119.0(2)	F(1S2)-C(2S)-S(2)	111.23(17)
C(11)-C(12)-H(12)	118.5(16)	O(2S3)-S(3)-O(3S3)	116.29(15)
C(13)-C(12)-H(12)	122.3(16)	O(3S3)-S(3)-O(1S3)	113.97(13)
C(14)-C(13)-C(12)	119.2(2)	O(2S3)-S(3)-C(3S)	103.46(13)
C(14)-C(13)-H(13)	122.1(18)	O(3S3)-S(3)-C(3S)	103.45(14)
C(12)-C(13)-H(13)	118.6(18)	O(1S3)-S(3)-C(3S)	102.81(12)
C(13)-C(14)-C(15)	119.0(2)	F(1S3)-C(3S)-F(3S3)	107.4(2)
C(13)-C(14)-H(14)	124.2(17)	F(1S3)-C(3S)-F(2S3)	107.5(2)
C(15)-C(14)-H(14)	116.8(18)	F(3S3)-C(3S)-F(2S3)	107.7(2)
N(3)-C(15)-C(14)	122.3(2)	F(1S3)-C(3S)-S(3)	112.27(18)
N(3)-C(15)-H(15)	116.5(14)	F(3S3)-C(3S)-S(3)	111.2(2)
C(14)-C(15)-H(15)	121.1(14)	F(2S3)-C(3S)-S(3)	110.53(18)
N(2)-C(16)-C(17)	109.57(17)		
N(2)-C(16)-H(16A)	106.4(14)		
C(17)-C(16)-H(16A)	109.8(14)		
N(2)-C(16)-H(16B)	110.6(16)		
C(17)-C(16)-H(16B)	110.5(16)		
H(16A)-C(16)-H(16B)	110(2)		
N(4)-C(17)-C(18)	121.73(19)		
N(4)-C(17)-C(16)	115.64(17)		
C(18)-C(17)-C(16)	122.63(19)		
C(17)-C(18)-C(19)	118.9(2)		
C(17)-C(18)-H(18)	117.8(15)		
C(19)-C(18)-H(18)	123.3(15)		
C(20)-C(19)-C(18)	119.2(2)		
C(20)-C(19)-H(19)	121.5(16)		
C(18)-C(19)-H(19)	119.2(16)		
C(21)-C(20)-C(19)	118.9(2)		
C(21)-C(20)-H(20)	122(2)		
C(19)-C(20)-H(20)	119(2)		
N(4)-C(21)-C(20)	122.2(2)		
N(4)-C(21)-H(21)	116.5(14)		
C(20)-C(21)-H(21)	121.1(14)		
N(1)-C(22)-H(22A)	108.4(13)		
N(1)-C(22)-H(22B)	108.2(15)		
H(22A)-C(22)-H(22B)	110(2)		
N(1)-C(22)-H(22C)	110.7(15)		
H(22A)-C(22)-H(22C)	107(2)		
H(22B)-C(22)-H(22C)	112(2)		
N(2)-C(23)-H(23A)	108.7(14)		
N(2)-C(23)-H(23B)	105.8(16)		
H(23A)-C(23)-H(23B)	112(2)		
N(2)-C(23)-H(23C)	108.6(15)		

Hydrogen bonds for [2.(H₂O)(OTf)]⁺ [Å and deg.].

D-H...A	d(D-H)	d(H...A)	d(D...A)	<(DHA)
O(1)-H(1O)...O(1S3) ^{#1}	0.80(3)	1.99(3)	2.786(3)	174(3)
O(1)-H(2O)...O(2S2)	0.68(3)	2.13(3)	2.801(3)	167(3)

Symmetry transformations used to generate equivalent atoms: #1 x+1,y,z

Table S5. Computed Metrical Parameters for **[2.(H₂O)(OTf)]⁺**

Cu	4.970392	3.881470	3.183078	H	7.694586	-1.213895	3.696675
Cu	3.084828	4.102674	4.843946	C	7.253413	0.626943	4.736680
S	3.255075	5.256675	2.967535	H	7.834969	0.397738	5.622228
O	6.645838	5.111121	3.764058	C	6.572209	1.836404	4.650776
H	6.688254	5.999664	3.372963	H	6.624306	2.568237	5.448731
H	6.586840	5.263807	4.737898	C	0.921587	2.374231	4.878555
N	5.145420	3.293221	1.202304	H	1.161783	1.999471	3.877709
N	1.021379	3.856542	4.845251	H	-0.097243	2.046186	5.120137
N	5.831202	2.173345	3.578989	C	1.915278	1.813277	5.868561
N	3.086144	2.488053	5.951942	C	1.662407	0.685250	6.642510
C	2.208306	4.207280	1.942639	H	0.712573	0.169626	6.550756
C	2.695233	3.686406	0.726708	C	2.636992	0.246323	7.538708
C	1.832206	2.954628	-0.096655	H	2.461942	-0.632047	8.151483
H	2.219094	.555379	-1.031206	C	3.825726	0.966834	7.652371
C	0.494885	2.723814	0.244559	H	4.598074	0.678773	8.356190
C	0.047648	3.215813	1.474556	C	4.006647	2.085205	6.846690
H	-0.976893	3.022780	1.783408	H	4.901616	2.691533	6.920091
C	0.878505	3.950862	2.329391	C	6.496667	3.606395	0.677545
C	4.126810	3.890289	0.284824	H	6.622045	4.690378	0.633906
H	4.362297	4.957602	0.226465	H	7.257672	3.194036	1.341888
H	4.260176	3.468728	-0.719906	H	6.633109	3.187925	-0.328644
C	0.327018	4.432552	3.652472	C	0.426451	4.442428	6.071352
H	-0.742454	4.191495	3.710486	H	-0.648748	4.224555	6.126067
H	0.425251	5.519043	3.740666	H	0.577036	5.524041	6.061003
C	-0.428176	1.971577	-0.684376	H	0.917903	4.032736	6.955498
H	0.096292	1.155042	-1.190834	S	4.940835	6.094753	6.911200
H	-0.824736	2.636128	-1.462825	F	5.083585	7.548442	4.707540
H	-1.281732	1.551676	-0.144164	F	6.082793	8.427326	6.430303
C	4.974165	1.823900	1.345842	F	3.908836	8.444033	6.307549
H	3.912668	1.626400	1.530868	O	3.674448	5.493163	6.389590
H	5.255221	1.295258	0.426267	O	6.168848	5.387671	6.446001
C	5.784053	1.327865	2.521408	O	4.914872	6.423776	8.343521
C	6.440050	0.101016	2.534912	C	5.008738	7.736396	6.039494
H	6.384110	-0.551486	1.670323				
C	7.175742	-0.261474	3.664117				

Table S6. NBO analysis of the Cu-Cu bond in $[2.\text{(H}_2\text{O)}(\text{OTf})]^+$ and comparison [1].

Cu-Cu distance (Å)	Wiberg bond index	Natural Bond Orbital composition	Occupancy	Bond order
		58.72% Cu1 (5.90% 4s, 0.81% 4p, 93.28% 3d)		
$[2.\text{(H}_2\text{O)}(\text{OTf})]^+$	0.39	41.28% Cu2 (36.68% 4s, 2.78% 4p, 60.53% 3d)	0.915	0.458
2.56				
		50.4% Cu1 (51.2% 4s, 5.6% 4p, 43.2% 3d)		
[1]	0.40	49.6% Cu2 (49.7% 4s, 5.6% 4p, 44.7% 3d)	0.802	0.466
2.58				

Table S7. Optical properties of relevant mixed-valent dinuclear copper systems.

Compound	λ_{\max} nm (ϵ ($M^{-1} \cdot cm^{-1}$))	d Cu...Cu (Å)
$[2.\text{(H}_2\text{O)}(\text{OTf})]^+$	1252 (690); 790 (735); 479 (525, sh); 425 (670, sh)	2.57
[1]	1115 (1190); 816 (1650), 537 (1050)	2.58
$[\text{Cu}_2(\text{XDK})(\text{i-OTf})\text{-}(\text{THF})_2], [\text{Cu}_2(\text{XDK})(\text{i-O}_2\text{CCF}_3)\text{-}(\text{THF})_2], [\text{Cu}_2(\text{XDK})(\text{THF})_4](\text{BF}_4)$	See ²⁴ and ref therein	2.40-2.42
$[\text{Cu}_2(i\text{PrdacoS})_2]^{+,\text{25}}$	1466(1200); 786 (sh); 602 (800); 358 (2700)	2.93
CuA^{25}	780-810 (2900-1600); 534-532(5300-3000); 480 (5200-3000); 350-363 (1200, sh)	2.4-2.6

Table S8. Predicted TD-DFT transitions (energies and intensities) and assignments for the calculated doublet state of $[2.\text{(H}_2\text{O)}(\text{OTf})]^+$.

Transition (MO number)	λ (nm)	Energy (cm ⁻¹)	Oscillator strength, f	Assignment
(1) β HOMO (205) → β LUMO (206)	1205	8298	0.0268	$\psi \rightarrow \psi^*$
(2) β HOMO-2 (203) → β LUMO (206)	758	13192	0.0761	LMCT
(3) β HOMO-12 (192) → β LUMO (206)	452	22124	0.0268	LMCT

Table S9. Bond lengths [Å] and angles [deg] for [3.(μOH)(OTf)₂].

Cu(1)-O(3)	1.915(3)	C(17)-C(18)	1.384(5)	N(2)-Cu(2)-Cu(1)	136.10(8)
Cu(1)-N(3)	2.017(3)	C(18)-C(19)	1.384(5)	O(1S2)-Cu(2)-Cu(1)	111.01(7)
Cu(1)-N(1)	2.027(3)	C(18)-H(18)	0.9500	S(1)-Cu(2)-Cu(1)	50.68(2)
Cu(1)-O(1S1)	2.313(3)	C(19)-C(20)	1.369(6)	C(1)-S(1)-Cu(1)	95.85(11)
Cu(1)-S(1)	2.3242(9)	C(19)-H(19)	0.9500	C(1)-S(1)-Cu(2)	95.32(11)
Cu(1)-Cu(2)	2.9447(6)	C(20)-C(21)	1.380(5)	Cu(1)-S(1)-Cu(2)	78.56(3)
Cu(2)-O(3)	1.926(3)	C(20)-H(20)	0.9500	C(11)-N(3)-Cu(1)	115.1(2)
Cu(2)-N(4)	2.009(3)	C(21)-H(21)	0.9500	C(15)-N(3)-Cu(1)	125.4(3)
Cu(2)-N(2)	2.056(3)	C(22)-H(22A)	0.9800	C(17)-N(4)-C(21)	119.3(3)
Cu(2)-O(1S2)	2.271(2)	C(22)-H(22B)	0.9800	C(17)-N(4)-Cu(2)	114.0(2)
Cu(2)-S(1)	2.3268(9)	C(22)-H(22C)	0.9800	C(21)-N(4)-Cu(2)	126.7(3)
S(1)-C(1)	1.786(3)	C(23)-H(23A)	0.9800	C(6)-C(1)-C(2)	120.2(3)
O(3)-H(3O)	0.9500	C(23)-H(23B)	0.9800	C(6)-C(1)-S(1)	120.1(3)
N(1)-C(10)	1.480(5)	C(23)-H(23C)	0.9800	C(2)-C(1)-S(1)	119.7(3)
N(1)-C(22)	1.485(5)	S(11)-O(2S1)	1.442(3)	C(3)-C(2)-C(1)	118.6(3)
N(1)-C(7)	1.493(4)	S(11)-O(3S1)	1.442(3)	C(3)-C(2)-C(7)	121.3(3)
N(2)-C(23)	1.483(4)	S(11)-O(1S1)	1.449(3)	C(1)-C(2)-C(7)	120.0(3)
N(2)-C(16)	1.493(4)	S(11)-C(1S)	1.813(4)	C(4)-C(3)-C(2)	122.0(3)
N(2)-C(8)	1.499(4)	F(1S1)-C(1S)	1.339(4)	C(4)-C(3)-H(3)	119.0
N(3)-C(11)	1.338(5)	F(2S1)-C(1S)	1.335(4)	C(2)-C(3)-H(3)	119.0
N(3)-C(15)	1.350(4)	F(3S1)-C(1S)	1.327(4)	C(3)-C(4)-C(5)	118.1(3)
N(4)-C(17)	1.341(5)	S(12)-O(2S2)	1.430(3)	C(3)-C(4)-C(9)	120.8(4)
N(4)-C(21)	1.347(4)	S(12)-O(3S2)	1.432(3)	C(5)-C(4)-C(9)	121.1(4)
C(1)-C(6)	1.393(5)	S(12)-O(1S2)	1.453(2)	C(4)-C(5)-C(6)	121.8(3)
C(1)-C(2)	1.408(5)	S(12)-C(2S)	1.814(4)	C(4)-C(5)-H(5)	119.1
C(2)-C(3)	1.396(5)	F(1S2)-C(2S)	1.324(4)	C(6)-C(5)-H(5)	119.1
C(2)-C(7)	1.500(5)	F(2S2)-C(2S)	1.324(4)	C(1)-C(6)-C(5)	119.0(3)
C(3)-C(4)	1.385(5)	F(3S2)-C(2S)	1.329(5)	C(1)-C(6)-C(8)	121.0(3)
C(3)-H(3)	0.9500	O(3)-Cu(1)-N(3)	92.60(12)	C(5)-C(6)-C(8)	119.9(3)
C(4)-C(5)	1.389(5)	O(3)-Cu(1)-N(1)	166.78(12)	N(1)-C(7)-C(2)	114.9(3)
C(4)-C(9)	1.515(5)	N(3)-Cu(1)-N(1)	81.45(12)	N(1)-C(7)-H(7A)	108.5
C(5)-C(6)	1.394(5)	O(3)-Cu(1)-O(1S1)	88.64(11)	C(2)-C(7)-H(7A)	108.5
C(5)-H(5)	0.9500	N(3)-Cu(1)-O(1S1)	96.11(11)	N(1)-C(7)-H(7B)	108.5
C(6)-C(8)	1.500(5)	N(1)-Cu(1)-O(1S1)	103.67(11)	C(2)-C(7)-H(7B)	108.5
C(7)-H(7A)	0.9900	O(3)-Cu(1)-S(1)	87.60(8)	H(7A)-C(7)-H(7B)	107.5
C(7)-H(7B)	0.9900	N(3)-Cu(1)-S(1)	164.28(9)	N(2)-C(8)-C(6)	114.3(3)
C(8)-H(8A)	0.9900	N(1)-Cu(1)-S(1)	94.95(8)	N(2)-C(8)-H(8A)	108.7
C(8)-H(8B)	0.9900	O(1S1)-Cu(1)-S(1)	99.60(7)	C(6)-C(8)-H(8A)	108.7
C(9)-H(9A)	0.9800	O(3)-Cu(1)-Cu(2)	40.07(8)	N(2)-C(8)-H(8B)	108.7
C(9)-H(9B)	0.9800	N(3)-Cu(1)-Cu(2)	123.38(9)	C(6)-C(8)-H(8B)	108.7
C(9)-H(9C)	0.9800	N(1)-Cu(1)-Cu(2)	136.11(8)	H(8A)-C(8)-H(8B)	107.6
C(10)-C(11)	1.496(5)	O(1S1)-Cu(1)-Cu(2)	108.06(7)	C(4)-C(9)-H(9A)	109.5

C(10)-H(10A)	0.9900	S(1)-Cu(1)-Cu(2)	50.76(2)	C(4)-C(9)-H(9B)	109.5
C(10)-H(10B)	0.9900	O(3)-Cu(2)-N(4)	91.58(12)	H(9A)-C(9)-H(9B)	109.5
C(11)-C(12)	1.378(5)	O(3)-Cu(2)-N(2)	166.29(11)	C(4)-C(9)-H(9C)	109.5
C(12)-C(13)	1.362(6)	N(4)-Cu(2)-N(2)	82.31(11)	H(9A)-C(9)-H(9C)	109.5
C(12)-H(12)	0.9500	O(3)-Cu(2)-O(1S2)	95.24(11)	H(9B)-C(9)-H(9C)	109.5
C(13)-C(14)	1.365(7)	N(4)-Cu(2)-O(1S2)	99.52(11)	N(1)-C(10)-C(11)	109.9(3)
C(13)-H(13)	0.9500	N(2)-Cu(2)-O(1S2)	97.87(10)	N(1)-C(10)-H(10A)	109.7
C(14)-C(15)	1.389(6)	O(3)-Cu(2)-S(1)	87.28(8)	C(11)-C(10)-H(10A)	109.7
C(14)-H(14)	0.9500	N(4)-Cu(2)-S(1)	164.32(9)	N(1)-C(10)-H(10B)	109.7
C(15)-H(15)	0.9500	N(2)-Cu(2)-S(1)	95.29(8)	C(11)-C(10)-H(10B)	109.7
C(16)-C(17)	1.508(5)	O(1S2)-Cu(2)-S(1)	96.16(7)	H(10A)-C(10)-H(10B)	108.2
C(16)-H(16A)	0.9900	O(3)-Cu(2)-Cu(1)	39.81(8)	N(3)-C(11)-C(12)	121.8(4)
C(16)-H(16B)	0.9900	N(4)-Cu(2)-Cu(1)	122.33(9)	N(3)-C(11)-C(10)	113.7(3)
C(12)-C(11)-C(10)	124.3(4)	F(2S1)-C(1S)-F(1S1)	106.9(3)	N(1)-C(22)-H(22C)	109.5
C(13)-C(12)-C(11)	119.6(4)	F(3S1)-C(1S)-S(11)	112.4(3)	H(22A)-C(22)-H(22C)	109.5
C(13)-C(12)-H(12)	120.2	F(2S1)-C(1S)-S(11)	110.9(3)	H(22B)-C(22)-H(22C)	109.5
C(11)-C(12)-H(12)	120.2	F(1S1)-C(1S)-S(11)	111.0(3)	N(2)-C(23)-H(23A)	109.5
C(12)-C(13)-C(14)	118.9(4)	O(2S2)-S(12)-O(3S2)	116.82(18)	N(2)-C(23)-H(23B)	109.5
C(12)-C(13)-H(13)	120.5	O(2S2)-S(12)-O(1S2)	114.06(16)	H(23A)-C(23)-H(23B)	109.5
C(14)-C(13)-H(13)	120.5	O(3S2)-S(12)-O(1S2)	113.93(15)	N(2)-C(23)-H(23C)	109.5
C(13)-C(14)-C(15)	120.2(4)	O(2S2)-S(12)-C(2S)	103.05(19)	H(23A)-C(23)-H(23C)	109.5
C(13)-C(14)-H(14)	119.9	O(3S2)-S(12)-C(2S)	104.30(18)	H(23B)-C(23)-H(23C)	109.5
C(15)-C(14)-H(14)	119.9	O(1S2)-S(12)-C(2S)	102.26(18)	O(2S1)-S(11)-O(3S1)	116.43(17)
N(3)-C(15)-C(14)	120.2(4)	S(12)-O(1S2)-Cu(2)	130.50(14)	O(2S1)-S(11)-O(1S1)	114.34(17)
N(3)-C(15)-H(15)	119.9	F(1S2)-C(2S)-F(2S2)	108.0(3)	O(3S1)-S(11)-O(1S1)	114.77(17)
C(14)-C(15)-H(15)	119.9	F(1S2)-C(2S)-F(3S2)	107.2(3)	O(2S1)-S(11)-C(1S)	103.74(18)
N(2)-C(16)-C(17)	109.8(3)	F(2S2)-C(2S)-F(3S2)	106.2(4)	O(3S1)-S(11)-C(1S)	102.83(17)
N(2)-C(16)-H(16A)	109.7	F(1S2)-C(2S)-S(12)	111.3(3)	O(1S1)-S(11)-C(1S)	102.05(18)
C(17)-C(16)-H(16A)	109.7	F(2S2)-C(2S)-S(12)	112.7(3)	S(11)-O(1S1)-Cu(1)	141.51(17)
N(2)-C(16)-H(16B)	109.7	F(3S2)-C(2S)-S(12)	111.2(3)	F(3S1)-C(1S)-F(2S1)	108.1(3)
C(17)-C(16)-H(16B)	109.7			F(3S1)-C(1S)-F(1S1)	107.2(3)
H(16A)-C(16)-H(16B)	108.2				
N(4)-C(17)-C(18)	121.6(3)				
N(4)-C(17)-C(16)	113.9(3)				
C(18)-C(17)-C(16)	124.5(3)				
C(19)-C(18)-C(17)	118.9(4)				
C(19)-C(18)-H(18)	120.5				
C(17)-C(18)-H(18)	120.5				
C(20)-C(19)-C(18)	119.3(4)				
C(20)-C(19)-H(19)	120.3				
C(18)-C(19)-H(19)	120.3				
C(19)-C(20)-C(21)	119.4(4)				
C(19)-C(20)-H(20)	120.3				
C(21)-C(20)-H(20)	120.3				
N(4)-C(21)-C(20)	121.5(4)				
N(4)-C(21)-H(21)	119.3				
C(20)-C(21)-H(21)	119.3				
N(1)-C(22)-H(22A)	109.5				
N(1)-C(22)-H(22B)	109.5				
H(22A)-C(22)-H(22B)	109.5				

References

1. Torelli, S.; Orio, M.; Pécaut, J.; Jamet, H.; Le Pape, L.; Ménage, S. *Angew. Chem. Int. Ed.* **2010**, *49* (44), 8249-8252.
2. Stoll, S.; Schweiger, A. *J. Magn. Res.* **2006**, *178*, 42.
3. Frisch, M. J. T., G. W.; Schlegel, H. B.; Scuseria, G. E.; Robb, M. A.; Cheeseman, J. R.; Zakrzewski, V. G.; Montgomery, J. A.; Stratmann, J. R. E.; Burant, J. C.; Dapprich, S.; Millam, J. M.; Daniels, A. D.; Kudin, K. N.; Strain, M. C.; Farkas, O.; Tomasi, J.; Barone, V.; Cossi, M.; Cammi, R.; Mennucci, B.; Pomelli, C.; Adamo, C.; Clifford, S.; Ochterski, J.; Petersson, G.; Ayala, A. P. Y.; Cui, Q.; Morokuma, K.; Malick, D. K.; Rabuck, A. D.; Raghavachari, K.; Foresman, J. B.; Cioslowski, J.; Ortiz, J. V.; Baboul, A. G.; Stefanov, B. B.; Liu, G.; Liashenko, A.; Piskorz, P.; Komaromi, I.; Gomperts, R.; Martin, R. L.; Fox, D. J.; Keith, T.; Al-Laham, M. A.; Peng, C. Y.; Nanayakkara, A.; Challacombe, M.; Gill, P. M. W.; Johnson, B.; Chen, W.; Wong, M. W.; Andres, J. L.; Gonzalez, C.; Head-Gordon, M.; Pople, J. A. *Gaussian09 2009, Revision A.02*, Gaussian Inc.: Pittsburg PA., 2003.
4. Becke, A. D. *J. Chem. Phys.* **1993**, *98* (7), 5648-5652.
5. Lee, C.; Yang, W.; Parr, R. G. *Physical Review B* **1988**, *37* (2), 785-789.
6. Hariharan, P. C.; Pople, J. A. *Theoret. Chim. Acta* **1973**, *28* (3), 213-222.
7. Hariharan, P. C.; Pople, J. A. *Mol. Phys.* **1974**, *27* (1), 209-214.
8. Reed, A. E.; Curtiss, L. A.; Weinhold, F. *Chem. Rev.* **1988**, *88* (6), 899-926.
9. Wiberg, K. B. *Tetrahedron* **1968**, *24* (3), 1083-1096.
10. Schafer, A.; Huber, C.; Ahlrichs, R. *J. Chem. Phys.* **1994**, *100* (8), 5829-5835.
11. Krishnan, R.; Binkley, J. S.; Seeger, R.; Pople, J. A. *The Journal of Chemical Physics* **1980**, *72* (1), 650-654.
12. Boys, S. F.; Bernardi, F. *Mol. Phys.* **1970**, *19* (4), 553-566.
13. Simon, S.; Duran, M.; Dannenberg, J. J. *The Journal of Chemical Physics* **1996**, *105* (24), 11024-11031.
14. Casida, M. E. *Recent Advances in Density Functional Methods* (Chong, D.P World Scentific: Singapore **1995**.).
15. Stratmann, R. E.; Scuseria, G. E.; Frisch, M. J. *J. Chem. Phys.* **1998**, *109* (19), 8218-8224.
16. Barone, V.; Cossi, M.; Tomasi, J. *J. Chem. Phys.* **1997**, *107* (8), 3210-3221.
17. Barone, V.; Cossi, M.; Tomasi, J. *J. Comput. Chem.* **1998**, *19* (4), 404-417.
18. Miertuš, S.; Scrocco, E.; Tomasi, J. *Chem. Phys.* **1981**, *55* (1), 117-129.
19. Tomasi, J.; Mennucci, B.; Cancès, E. *Journal of Molecular Structure: THEOCHEM* **1999**, *464* (1-3), 211-226.
20. Neese, F. *Wiley Interdiscip. Rev. Comput. Mol. Sci.* **2012**, *2* (1), 73-78.
21. Pantazis, D. A.; Chen, X.-Y.; Landis, C. R.; Neese, F. *J. Chem. Theory Comput.* **2008**, *4* (6), 908-919.
22. Pantazis, D. A.; Neese, F. *J. Chem. Theory Comput.* **2009**, *5* (9), 2229-2238.
23. chemcraft <http://chemcraftprog.com>.
24. LeCloux, D. D.; Davydov, R.; Lippard, S. J. *Inorg. Chem.* **1998**, *37* (26), 6814-6826.
25. Houser, R. P.; Young, V. G.; Tolman, W. B. *J. Am. Chem. Soc.* **1996**, *118* (8), 2101-2102.